Durham University

Durham E-Theses

Investigating the Interplay Between Cytolinkers and Nesprin-3

LANA FAIDULLA

How to cite:

FAIDULLA, LANA (2021) Investigating the Interplay Between Cytolinkers and Nesprin-3. Masters thesis, Durham University.

Use policy

The full-text may be used and/or reproduced, and given to third parties in any format or medium, without prior permission or charge, for personal research or study, educational, or not-for-profit purposes provided that:

- a full bibliographic reference is made to the original source
- a https://etheses.durham.ac.uk/id/eprint/14075/ is made to the metadata record in Durham E-Theses
- the full-text is not changed in any way

The full-text must not be sold in any format or medium without the formal permission of the copyright holders.

Please consult the full Durham E-Theses policy for further details.

Academic Support Office, The Palatine Centre, Durham University, Stockton Road, Durham, DH1 3LE
e-mail: e-theses.admin@durham.ac.uk Tel: +44 0191 334 6107
https://etheses.durham.ac.uk

Investigating the Interplay Between Cytolinkers and Nesprin-3

Lana Faidulla

St Aidan's College

Supervisors: Dr Iakowos Karakesisoglou and Dr Martin Goldberg

Submitted for the qualification of Master of Science

Department of Biosciences, Durham University

December 2020

Abstract

The mammalian cytoskeleton is a complex and dynamic network of proteins which function to organise contents of cells, allow cells to respond to external environments, change shape and become motile. Cytoskeletal proteins interact and work with many other proteins in the cytoplasm and nucleus including microtubule actin cross-linking factor 1 (MACF1), plectin and nesprin-3 to achieve these roles. MACF1 is a spectraplakin protein, able to bind all three elements of the cytoskeleton: actin, microtubules and intermediate filaments, linking different cytoskeletal networks together. Through alternative splicing, plectin is expressed as 11 different isoforms and is primarily an intermediate filament binding protein, anchoring intermediate filaments to desmosomes and hemidesmosomes. Nesprin-3 is a member of the LINC complex (Linker of Nucleoskeleton and Cytoskeleton) family of proteins and binds with plectin's actin-binding domain, establishing a link between the outer nuclear membranes with intermediate filaments.

The relationship between nesprin-3, MACF1a3 (the third isoform of MACF1, produced by alternative splicing) and plectin was investigated using western blotting, immunofluorescence and transfection techniques. Results of these experiments demonstrated that MACF1a3 and nesprin-3 were expressed in varying levels within COS-7, HaCaT, C6 and HDF cells. Overexpression of wild-type nesprin-3α did not promote MACF1a3 recruitment to the nuclear envelope but did result in plectin recruitment to the nuclear envelope. Nesprin-3 mutation constructs H222Y and A927E also recruited plectin to the nuclear envelope.

Table of Contents

List of Figures

List of Tables

Abbreviations

ACF7: Actin Cross-Linking Factor 7

ARCA-1: Autosomal recessive cerebellar ataxia type I

BPAG1: Bullous pemphigoid antigen 1

CH domain: Calponin homology domain

EBS-MD: epidermolysis bullosa simplex associated with muscular dystrophy

ECM: Extracellular matrix

EMT: Epithelial-mesenchymal transition

GSK3β: glycogen synthase kinase 3 beta

HNSCC: Head and Neck Squamous Cell Carcinoma

IF: Intermediate filament

INM: Inner nuclear membrane

KASH: Klarsicht/ANC-1/SYNE homology

LINC: Linker of Nucleoskeleton and Cytoskeleton

MAP: Microtubule-associated proteins

MACF1: Microtubule Actin Cross-Linking Factor 1

MACF1a1: Microtubule Actin Cross-Linking Factor 1 isoform 1

MACF1a2: Microtubule Actin Cross-Linking Factor 1 isoform 2

MACF1a3: Microtubule Actin Cross-Linking Factor 1 isoform 3

ONM: Outer nuclear membrane

PA-JEB: Pyloric atresia associated with junctional epidermolysis bullosa

WT: Wild-type

Declaration

I confirm that all the research presented in this thesis is my own work unless it has been otherwise referenced in the text. The material contained in the thesis has not been previously been submitted for a degree in this or any other institution.

Statement of Copyright

“The copyright of this thesis rests with the author. No quotation from it should be published without the author's prior written consent and information derived from it should be acknowledged.”

Acknowledgments

I would firstly like to thank my supervisor, Dr Iakowos Karakesisoglou, for allowing me to experience and carry out research in his laboratory and for his constant patience and encouragement. Thank you for always pushing me to do better and for not allowing me to feel discouraged when things weren't going the way we wanted (as they frequently did!).

I would also like to thank my second supervisor, Dr Martin Goldberg and my lab partners, Eve and Kleopatra for all their great help and advice throughout my project.

Next, I would like to thank my amazingly supportive friends. To Tommy, for being the best non-lab partner I could have asked for, for his constant humour and wit, and for making the entire experience so much more fun. To Bethany and Olivia, for all the pep talks and for being so supportive always. To Muzz, for always listening to me whinge and for the daily messages to push me to keep writing.

Finally, to my amazing family, this is for you. Thank you for the constant support and for never allowing me to give up, xoshm dawen.

1. Introduction

1.1 The dynamic cytoskeleton

The mammalian cytoskeleton is dynamic and serves many functions which allows it to organise the contents of cells, allow cells to adhere to each other and respond to external environments and stimuli enabling cells to change shape and become motile (Fuchs and Karakesisoglou, 2001). There are three main cytoskeletal polymers that enable the cells to carry out these roles: F-actin, microtubules and intermediate filaments. The polymers also provide cells with an elasticity that enables them to maintain and revert to their original shape following the release of external forces on them. This elasticity is achieved as the cells are filled with a three-dimensional filamentous network of cytoskeletal proteins.

The cytoskeleton also has a major mechanical role in linking the plasma membrane of the cell and interior membranes such as the endoplasmic reticulum to the rest of the cell (Pegoraro, Janmey and Weitz, 2017). The networks that are formed by the cytoskeletal polymers which allow for all of the functions above are controlled by several classes of regulatory proteins. These regulatory proteins include nucleation-promoting factors and capping proteins which initiate filament formation and stop filament growth respectively and depolymerising factors that promote disassembly of proteins. Cross-linkers and stabilising proteins are also involved in organising and reinforcing network structures (Fletcher and Mullins, 2010). Each of the cytoskeletal polymers have varying levels of stiffness and serve different purposes.

The stiffest cytoskeletal filaments are the microtubules (Bhushan, 2010), made up of α/β-tubulin heterodimers that are highly dynamic and have key roles in cell growth, mitosis and transport by providing molecular tracks for molecular motors to move and transport cargo across (Kodama et al., 2003). Microtubules are generally assembled by the microtubule organisation centre (MTOC), which contains γ-tubulin that works as a microtubule nucleator. Microtubules show dynamic instability that is characterised by sudden

switches from growing and growth arrest to quick depolymerisation. This dynamic behaviour is regulated by intrinsic and extrinsic factors. Two types of proteins which interact with microtubules are microtubule (+)-end-binding proteins (+TIP) and microtubule-associated proteins (MAP). These proteins have the ability to stabilise and destabilise microtubules, severe them or change polymerisation dynamics (Hohmann and Dehghani, 2019). One important class of MAPs are kinesin and dynein, motor proteins which serve as cargo transporters, transporting membrane components, intermediate filaments and their precursors and signalling molecules to name a few (Brown et al., 1996). Typically, microtubules play roles in transport as tracks, in spindle positioning during mitosis, migration and cell shape control. They also play key roles in cell division as they enable chromosomes to segregate during anaphase, the final step of mitosis.

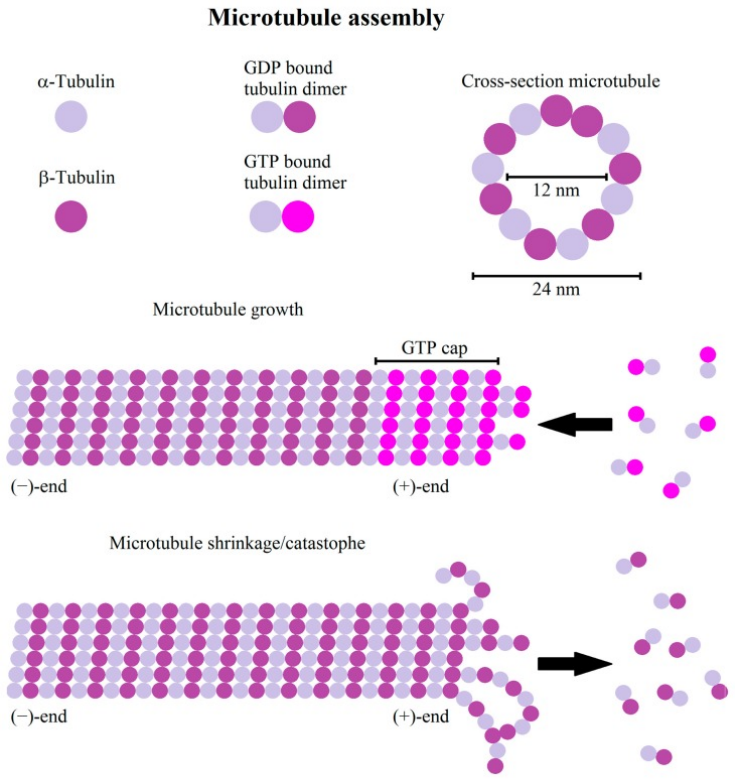

Figure 1 Schematic diagram showing microtubule elongation and shrinkage. Microtubules consist of α/β heterodimers. A hollow tube is formed and elongated by the addition of the heterodimers and a GTP-cap at the (+)-end is added to protect the microtubules from shrinkage. Microtubule shrinkage is induced when the (+)-end loses its GTP-cap. Figure acquired from (Hohmann and Dehghani, 2019).

Actin filaments are semi-flexible filaments when compared to microtubules and their remodelling allows for differentiation, division and membrane organisation. They are considered to be the most dynamic of the three cytoskeletal proteins as they are able to undergo structural changes in a matter of minutes, for example to determine the shape of a cell (Hohmann and Dehghani, 2019). Actin exists in two distinct states in cells, as monomeric G-actin and filamentous F-actin, as shown in Figure 2 (Hohmann and Dehghani, 2019). Actin filaments have a distinct polarity as all actin monomers are oriented in the same direction and have more and less dynamic sides, named (+)-end and (-)-end. The (+)-end has a polymerisation rate which is ten times higher than that of the (-)-end meaning that growth is promoted from the (+)-end (Pollard, 2016). Although actin is less stiff than microtubules, the presence of crosslinkers in high concentrations which bind to actin filaments produces an assembly of highly organised, stiff structures or networks. These networks

are involved in chemotaxis (cell movement towards a gradient of increasing concentration of a particular substance or chemical), cell-cell communication, phagocytosis and endocytosis. Furthermore, as actin filaments are polarised, they are able to serve as tracks for molecular motors which move in one direction. These motors, with regards to actin filaments, are members of the family of myosin proteins. They play roles in organising the actin cytoskeleton and can act on bundles of aligned actin filaments in stress fibres to enable the cells to contract and sense the external environment (Fletcher and Mullins, 2010).

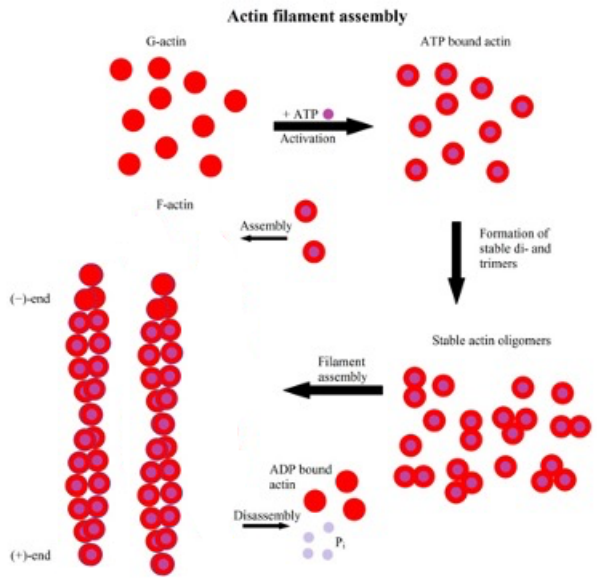

Figure 2 Schematic diagram showing F-actin formation. G-actin binds to ATP and forms stable dimers and trimers. At this stage, filament nucleation increases rapidly, and filaments are assembled to produce F-actin. ATP is hydrolysed to ADP at the (-)-end, causing F-actin disassembly back to G-actin. Figure modified from (Hohmann and Dehghani, 2019) to show correct orientation of F-actin with the +-end at the bottom where assembly is depicted.

Intermediate filaments (IFs) can be formed from a wide range of subunit proteins and can be characterised based on their localisation and composition (Fife, McCarroll and Kavallaris, 2014). By extending to the cytoplasmic interior, IFs coordinate cytoskeletal activities through information relay from the cell surface to inner components of the cell (Chang and Goldman, 2004). Proteins that are able to form IFs are a large protein class, are encoded by at least 70

genes and organise the filaments with a diameter of 10nm. IFs can be grouped into 5 classes depending on their structure and sequence homology and the first four classes represent cytoplasmic IFs. As a brief summary, keratins are type I and II IFs. Vimentin, desmin and peripherin are type III IFs. Type IV IFs are internexin, synemin and nestin. Type V IFs are nuclear filaments called lamins (Hohmann and Dehghani, 2019). Cytoplasmic IFs form dense meshworks in the perinuclear space which reach the cell cortex, but the structure and form of the networks depend on the type of IF. To maintain cell and tissue adhesion, IFs have been known to interact with desmosomes, hemidesmosomes and focal adhesion sites near the cell cortex (Hohmann and Dehghani, 2019). In addition, IF organisation is further influenced by the plakin family of proteins which connect IFs not only to microtubules and actin but also to the nucleus (Leung, Green and Liem, 2002). IF assembly is described in Figure 3.

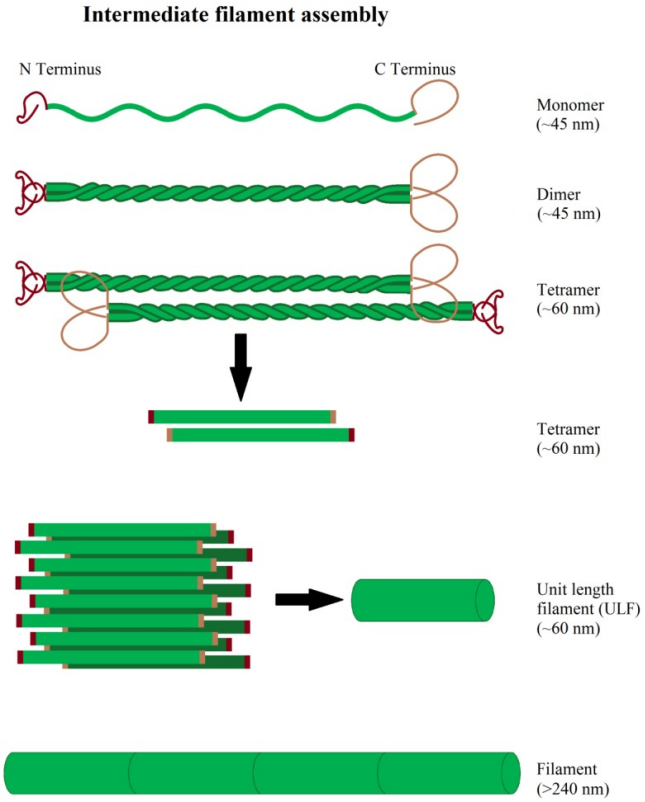

Figure 3 Schematic diagram showing the formation of intermediate filaments. Two monomers spiral around each other to produce a dimer. Two dimers aggregate to produce a tetramer and eight tetramers aggregiate to a unit length filament. The final filament is formed via end-to-end aggregation of unit filaments. This process does not require ATP or GTP, unlike F-actin and microtubule production. Figure acquired from (Hohmann and Dehghani, 2019).

There is increasing implication on the importance of crosstalk and interdependency of the cytoskeletal components in many diseases such as neurodegenerative disorders, cancer and cardiovascular diseases. Moreover, cytoskeletal protein abnormalities have been found to be the underlying causes of many disease phenotypes. Research into how cytoskeletal elements may be causing these disorders has yielded interested and medically useful results (Ramaekers and Bosman, 2004). Using cancer as one example, studies have shown that aberrant cell migration increases metastasis rates. Cells can initiate migration by extending actin polymerisation-driven cell membrane protrusions towards an extracellular cue, which are then stabilised by adhesions linking the actin cytoskeleton to the extracellular matrix (ECM) proteins (Fife, McCarroll and Kavallaris, 2014). This type of cell migration is also known as mesenchymal motility. Epithelial-mesenchymal transition (EMT) is one such well-studied model of dynamic reorganisation of the actin

cytoskeleton (Fife, McCarroll and Kavallaris, 2014). EMT is a biological process that allows an epithelial cell to undergo biochemical changes that enable it to assume a mesenchymal cell phenotype (Kalluri and Weinberg, 2009). Under normal circumstances, the epithelial cell would be interacting with the basement membrane through its basal surface but following EMT, the cell has enhanced migratory capacity, invasiveness and increased resistance to apoptosis. Type 3 EMT is the EMT associated with cancer progression and metastasis. Cytoskeletal components which have been implicated in this type of EMT in addition to actin include vimentin and desmin, type III IFs. Furthermore, carcinoma cells used in mouse studies which have acquired the EMT phenotype have been found to express mesenchymal markers like vimentin and desmin and are considered to be those cells which enter the subsequent invasion-metastasis cascade (Yang and Weinberg, 2008). This example provides one important reason why research into the cell cytoskeleton is so vital.

However, cytoskeletal proteins interact and work with many other proteins in the cytoplasm and nucleus. Some of these proteins belong to the family of plakins and spectraplakins.

1.2 The LINC Complex

The LINC complex (Linker of Nucleoskeleton and Cytoskeleton) is present in the nuclear envelope, connecting the lamina and cytoskeletal elements. The LINC complexes play key roles in many cellular functions such as cytoskeletal organisation, cellular division and organelle positioning.

Creating a barrier between the nucleus and the cytoplasm, the nuclear envelope possesses an inner and outer membrane, which are separated by a perinuclear space. As shown in Figure 6, the inner nuclear membrane (INM) contains specific proteins such as SUN1, SUN2, emerin and lamin A and B. Nesprins 1-4 are integrated at the outer nuclear membrane (ONM) via their C-terminal KASH (Klarsicht/ANC-1/SYNE homology) domain (Meinke, Nguyen and Wehnert, 2011; Janin et al., 2017). Sun1 and Sun2 contain N-terminal domains followed by a transmembrane spanning region, a luminal domain and a conserved region named the SUN domain. Sun proteins are widely expressed in tissues and have been identified as having roles in nuclear positioning, centrosome localisation and apoptosis. Their N-terminal also interacts with lamin A and B, which are essential for the localisation and retention of emerins to the INM (Ostlund et al., 2009).

Nesprins have N-terminal regions containing spectrin repeats and a conserved C-terminal KASH domain. Nesprins are encoded by five different genes which results in production of proteins of varying molecular weights: nesprin-1 and nesprin-2 have molecular weights of ~1000 kDa and ~800 kDa respectively, whereas nesprin-3 and nesprin-4 are lower molecular weight proteins with molecular weights of ~110 and 42 kDa respectively (Ostlund et al., 2009). Connecting cytoskeletal filaments to the nucleus allows for nuclear positioning and binding to actin filaments (Crisp et al., 2005). Furthermore, through the binding of plectin to nesprin-3, it has been shown that nesprin-3 links the nuclear envelope to cytoplasmic IFs. In summary, there are different ways by which each nesprin protein binds to a cytoskeletal linker protein. For example, nesprin-1 and -2 contain an N-terminal ABD which connects the nuclear envelope to the actin cytoskeleton whereas nesprin-3 and -4 bind to the cytoskeleton indirectly. This indirect binding involves the motor protein kinesin-

1 binding with nesprin-4 and therefore connecting the nuclear envelope with microtubules and plectin binding with nesprin-3 to mediate an interaction with intermediate filaments (Wilhelmsen et al., 2005).

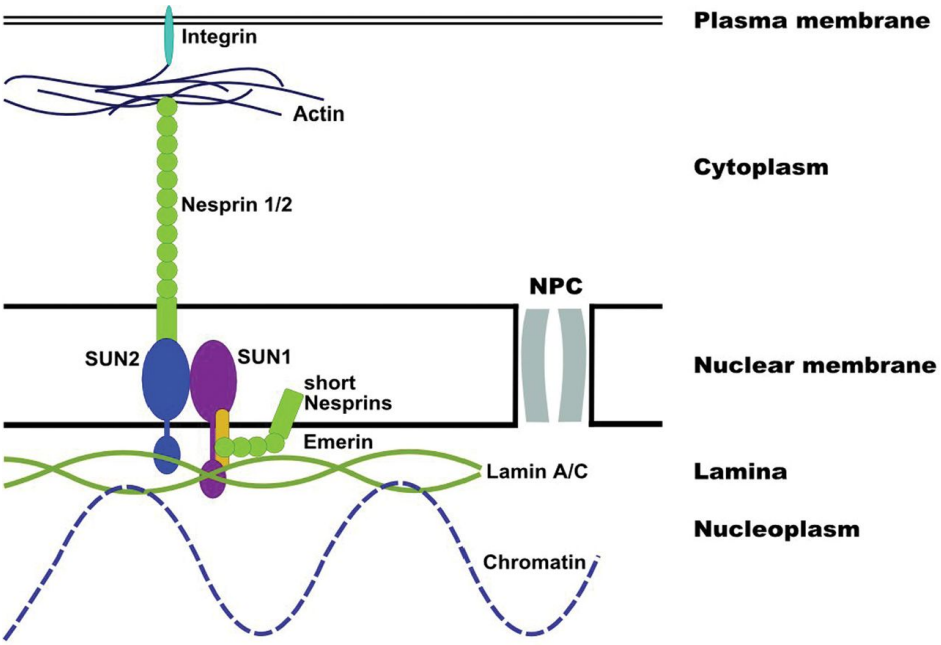

Figure 4 Schematic showing the LINC complex bridge and its components. SUN proteins of the inner nuclear membrane interact at the perinuclear space with Nesprin-1/2 of the outer nuclear membrane, resulting in the interaction of the nucleoskeletal and cytoskeletal networks. Acquired from Meinke, Nguyen and Wehnert, (2011).

1.2.1 Nesprin-3

Nesprin-3 was first identified in a yeast two-hybrid screen when Wilhelmsen et al., 2005 were looking for binding partners of plectin. Nesprin-3 is a highly conserved member of the nesprin family of proteins, and its gene encodes two isoforms: nesprin-3α and nesprin-3β. Nesprin-3α is made up of eight spectrin repeats and a C-terminal KASH domain which mediates the insertion of nesprin-3α into the outer nuclear membrane (Méjat, 2010). The nesprin-3β isoform however is the result of alternative mRNA splicing. There is a mouse nesprin-3β and zebrafish nesprin-3β form which differ from each other with regards to their composition. Mouse nesprin-3β lacks the first spectrin repeat whereas zebrafish nesprin-3β lacks seven amino acids in the first spectrin repeat (Ketema and Sonnenberg, 2011). Nesprin-3α binds to plectin through

plectin's ABD and via a motif on its N-terminal spectrin repeat, which nesprin-3β lacks, therefore disabling the isoform to bind plectin (Ketema et al., 2013).

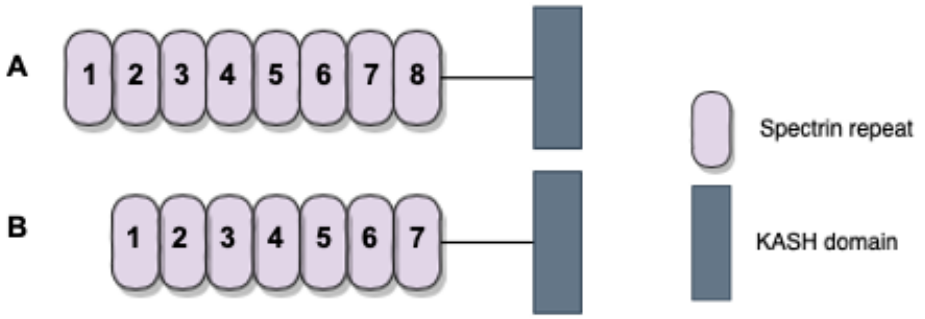

Figure 5 Schematic diagram of the domain structure of two nesprin-3 variants. Diagram shows the difference between the two known nesprin-3 variants: A) Nesprin-3α and B) Nesprin-3ß. Nesprin-3ß lacks one spectrin repeat.

1.3 Plakins

Mammalian plakins are a family of seven cytoskeletal proteins including MACF1, BPAG1, plectin, desmoplakin, envoplakin, periplakin and epiplakin (Quick, 2018). MACF1 is encoded for by the gene *MACF1*, one of the spectraplakin family's two mammalian genes and is also known as ACF7, macrophin and MACF (Hu et al., 2016). MACF1 and BPAG1 are able to perform crosslinking functions between actin and microtubules whereas plectin crosslinks intermediate filaments to microtubules. This will a parameter explored in this thesis. The structural organisation of plectin, periplakin, envoplakin and desmoplakin is less complex in contrast with MACF1 and BPAG1.

1.3.1 Spectraplakins

Spectraplakins are enormous, evolutionarily conserved cross-linkers (>500kDa). *MACF1* is a gene which expresses seven different isoforms of the spectraplakin protein MACF1 shown in Figure 1 (Hu et al., 2016). Spectraplakins enable some of their isoforms to regulate microtubules and co-ordinate linkages with the actin cytoskeleton and IFs. The isoforms achieve this dual binding through several binding domains in their N and C-termini. MACF1 isoforms 1 and 2 have one actin-binding domain (ABD) composed of two calponin homology (CH) domains, CH1 and CH2. Jefferson, Leung and Liem, (2004) suggest that a greater actin binding affinity is reached if both CH domains are present. Another common domain of the aforementioned isoforms is a variable in the number of spectrin repeats. MACF1 contains 23 spectrin repeats. Palmucci et al., (1994) suggest that the spectrin repeats give the proteins flexibility to respond to mechanical forces whilst acting to separate the N and C-termini. EF hand motifs and a GAR domain are found at the C-terminus. The EF hand domain changes to an open confirmation following calcium binding, amplifying its heterodimer binding partner β-spectrin's ABD function (Suozzi, Wu and Fuchs, 2012). The GAR domain's function is to associate to and stabilise microtubules, allowing spectraplakins to link them to other cytoskeletal network components. The final domain, named plakin, is thought to have originated from spectrin repeats and has key roles in linking the IF cytoskeleton and membrane-protein complexes to adhesive junctions (Suozzi, Wu and Fuchs, 2012; Jefferson, Leung and Liem, 2004).

Similarly to MACF1, transcripts of BPAG1 (bullous pemphigoid antigen 1a) also undergo alternative splicing, resulting in the production of different isoforms with different functional domains. One such isoform is BPAG1a.
MACF1a and BPAG1a have similar domain organisation, containing an actin-binding domain, a rod domain with spectrin repeats, a plakin domain and a C-terminus which can bind and stabilize microtubules (Karakesisoglou et al. 2000). Despite belonging to the spectraplakin family of proteins and having similar domain organisation, research into these proteins has demonstrated the difference in their functions. A study which has highlighted some of these

differences was carried out by Chen et al in 2006. They suggested that as MACF1 and BPAG1 are closely related members of the plakin family and are both expressed early in development, they would have overlapping functions. To test this, they compared MACF1+/− mice with *MACF1*−/− and *BPAG1*−/− mice. MACF1+/− mice appeared to be normal and fertile whereas *MACF1*−/− died in the early stages of embryogenesis. Contrastingly, *BPAG1*−/− mice survived until weaning but suffered from sensory neuron degeneration. This study suggests that BPAG1 and MACF1 do not have completely overlapping functions despite their structural similarities. Furthermore, it implies that BPAG1 is unable to compensate for MACF1 in *MACF1*−/− mice even though mRNAs of all BPAG1 isoforms were detected in the early stages of mouse embryogenesis (Chen, 2006).

1.3.2 Microtubule Actin Cross-Linking Factor 1: A spectraplakin protein

The *MACF1* gene is positioned on mouse chromosome 4 and human chromosome 1p34.3 and comprises more than 110 exons, spanning over 400 kb (Hu et al., 2016). MACF1 was first discovered by Byers *et al*. and was classed as a member of the spectraplakin family after discovering that the genes shared characteristics of plakin and spectrins, with identical gene sequences (Gong, Besirli and Lomax, 2001; Leung et al., 1999). Alternative splicing produces the various isoforms of MACF1 shown in Figure 6, each with a unique sequence of domains. The first three isoforms discovered (MACF1a1, MACF1a2 and MACF1a3) share similar features but have subtle differences in their structural makeup. The differences are in their N-termini: MACF1a1 and MACF1a2 are similar in their actin-binding domain structure but as Figure 6 shows, MACF1a2 has a longer N-terminus. MACF1a3 has a longer N-terminal domain but lacks a CH1 domain. (Jefferson, Leung and Liem, 2004) suggest that the presence of only the CH2 domain means that MACF1a3 has a weaker affinity for actin than if it only possessed the CH1 domain. They also suggested that the absence of the CH1 domain could abolish interactions with actin completely.

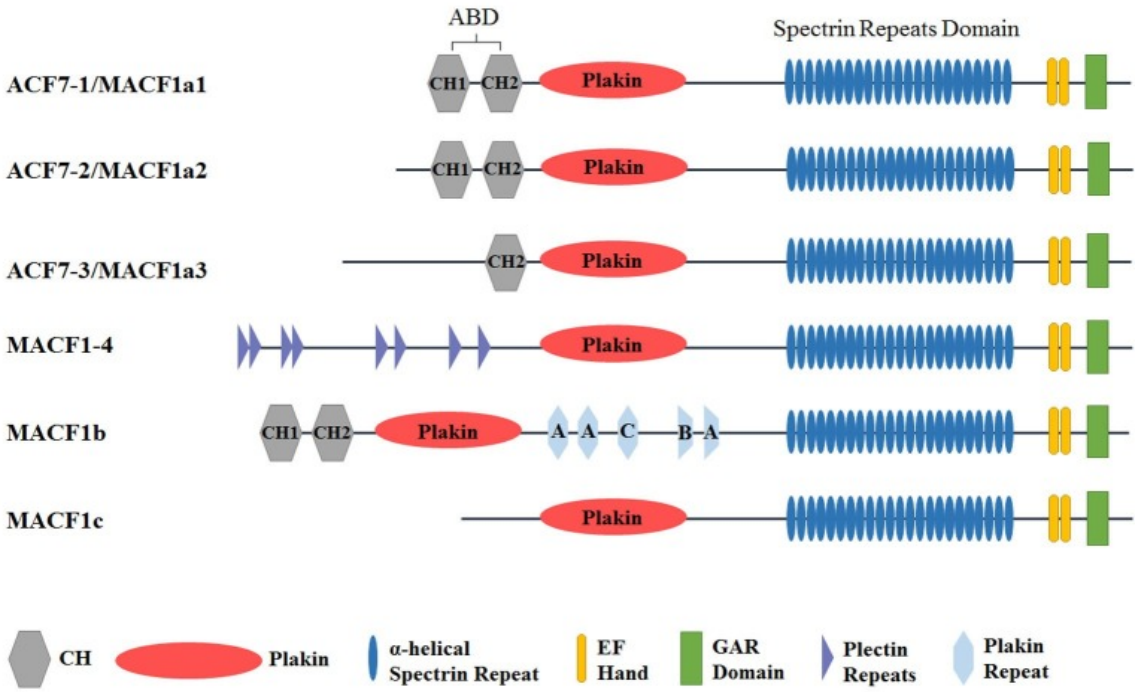

Figure 6 Domain structure of the six different isoforms of MACF1. Each isoform has a unique structure of domains. In total, there are six different types of domains: actin binding domain containing CH1 and CH2 fragments, a plakin domain, a spectrin repeats domain with 23 α-helical spectrin repeats, two EF hand motifs, a GAR domain, plectin repeat domains and plakin domain (A, B, C). Image acquired from (Hu et al, 2016).

As MACF1 is a cytoskeletal linker protein, it is expressed through all tissues with different distribution levels depending on the isoform (Bernier et al., 2000; Okuda et al., 1999). In human tissues, MACF1 is expressed widely in thyroid, skeletal muscle, heart, adrenal and pituitary glands amongst others (Okuda et al., 1999; Sun et al., 1999). In mouse tissues, MACF1 is also widely expressed and was shown by Bernier *et al.* to be present in the brain, spleen, liver, stomach, lungs, kidney and skin. Different isoform distributions are present in certain tissues. For example, MACF1a3 is expressed largely in the brain and spinal cord, with reduced levels in the lung and kidney. MACF1a1 however is found mostly in the skin and kidney. Some isoforms also appear before others in the early stages of embryonal development in mice. From day 7.5 to day 10.5, MACF1a1 mRNA can be detected. MACF1a2 mRNA however is only detectable at and after day 10.5 (Bernier et al., 2000). The importance of MACF1 expression in early embryo development was shown through a series

of experiments using MACF1 knockout mice lacking a primitive streak, node and mesoderm, causing the mice to die at the gastrulation stage (Chen, 2006).

Studies of MACF1 have demonstrated its involvement in human diseases, such as a novel myopathy named spectraplakinopathy type 1, and in cancers such as glioblastoma due to its roles in cell proliferation and cell signalling. Studies by Hu *et al.* showed that knockdown of MACF1 caused a halt in the allocation of microtubules and actin, distorting cell morphology, reducing levels of cell proliferation and inhibiting the cell cycle at S phase. In signalling pathways such as the Wnt/β-catenin pathways, MACF1 deficiency has been shown to cause downregulation of the Wnt/β-catenin pathways as it cannot interact with the co-receptor LRP5/6, preventing the movement of the Axin complex to the cell membrane. This deficiency results in a lack of vesicle transport to the cell periphery.

MACF1 is largely expressed in brain tissues and has recently been implicated in the promotion of glioblastomas in the brain. Afghani *et al.* demonstrated that downregulation of MACF1 inhibits the proliferation and migration of glioblastoma cells, making MACF1 a good diagnostic and prognostic indicator of glioblastoma. They also found that suppressing MACF1 led to downregulations in Wnt signalling pathway proteins such as Axin1 and β-catenin, leading once again to a reduction in the migration and proliferation of glioblastoma cells.

Research has also implicated MACF1 as one of the genes responsible for metastasis of breast carcinoma cells. The ErbB2 protein is involved in tumour cell metastasis, enhancing microtubule outgrowth to the cell cortex via a complex that includes Memo, the GTPase RhoA and formin mDia1. This causes breast cancer cells to form protrusions, occupied by outgrowing microtubules. ErbB2 can inhibit the phosphorylation of glycogen synthase kinase 3 beta (GSK3β), a known regulator of MACF1, allowing it to localise APC, which is a tumour suppressor gene, to the plasma membrane where it recruits MACF1. This action promotes the growth of microtubules and promotes their capture and stabilisation during breast carcinoma cell motility

(Zaoui et al., 2010; Yucel and Oro, 2011). As mentioned above, GSK3β is a known regulator of MACF1 and is an enzyme that is ubiquitously expressed in all cell and tissue types. It regulates many cellular functions, from cell proliferation and gene expression to cell architecture and neural development. When GSK3β is inhibited, it phosphorylates MACF1 and uncouples MACF1 from microtubules. This action takes place in the GAR domain where microtubule binding occurs. 32% of the amino acid residues in the GAR domain are serines or threonines, which are possible GSK3β phosphorylation sites (Krishnankutty et al., 2017)

In 2012, a novel myopathy later named spectraplakinopathy type 1 was discovered. A patient with skeletal muscle problems presented with hypotonia and pain. It was later shown that a single, duplicated region covering the MACF1 gene on chromosome 1p34.3 affected 4 major isoforms of MACF1, causing a reduction in MACF1 expression and internal structural changes of endothelial and satellite cells (Jørgensen et al., 2014).

1.3.3 Plectin

Plectin is a member of the plakin family and is a large (~500 kDa) and versatile linker of the cytoskeleton (Steinböck and Wiche, 1999). It has been shown to have the ability to interact with intermediate filaments, actin filaments and microtubules. Furthermore, plectin can also crosslink intermediate filaments with microtubule and actin filaments (Quick, 2018). It achieves this vast binding ability through its multidomain structure and alternative splicing, expressing it as 11 known isoforms. Although plectin can bind actin filaments and microtubules, primarily it is an IF binding protein and thus anchors IFs to cellular sites such as desmosomes and hemidesmosomes. Plectin's structure is similar to other proteins of the plakin family. It consists of an N-terminal domain which contains an actin-binding domain, a plakin domain with nine spectrin repeats, an SH3 domain and a central rod domain which is a 200nm long coiled coil. The C-terminal domain contains six plectin repeat domains and a linker region which contains the IF-binding domain (Castañón, Walko,

Winter and Wiche, 2013). Most plectin isoforms differ in their short N-terminal sequences which determine the cellular localisation of the isoforms and confer their tissue-specific expression (Rezniczek, 2003). For example, plectin isoform P1 is targeted to the nucleus and ER membrane, whereas another isoform, P1c is targeted to microtubules. Hence, plectin is a protein which is expressed in a vast variety of different tissues and cell types. This also includes plectin being found at plasma membrane attachment sites of IFs, microfilaments and focal adhesions (Castañón, Walko, Winter and Wiche, 2013).

Plectin has been implicated in many human diseases. Most commonly, a mutation in the plectin gene is the cause of autosomal recessive forms of the skin disease epidermolysis bullosa simplex associated with muscular dystrophy (EBS-MD). These patients lack plectin expression in their cells as a result of premature stop codons and nonsense-mediated mRNA decay (Gundesli et al., 2010). More recently, plectin upregulation has also been implicated in various types of cancers. A study by Katada et al. 2012 found that plectin is involved in the migration and invasion of Head and Neck Squamous Cell Carcinoma (HNSCC) and could be used as a novel prognostic marker for HNSCC. They found that plectin, amongst a group of other proteins that were expressed in HNSCC, was significantly overexpressed. Moreover, patients with a high plectin level had a declined survival rate due to more frequent recurrences of the cancer. They also showed that suppression and decreased expression of endogenous plectin inhibited the proliferation, migration and invasion of HNSCC cells (Katada et al., 2012).

Another manner by which plectin interacts with cytoskeletal elements such as microtubules is through its isoform P1c. In keratinocytes, P1c shows partial colocalization with microtubules. In addition to being able to bind microtubules, recent studies have shown that plectin, or lack of can also act as microtubule destabiliser. This study, by Valencia et al., 2013, showed that in P1c-deficient keratinocytes and plectin-null cells, microtubules tended to be more resistant to drug-induced disassembly. Therefore, increased microtubule stability due

to P1c deficiency resulted in altered cell shape, increased velocity but loss of directionality of migration and reduced growth rates of cells amongst others.

Plectin also interacts with Nesprin-3a, an outer nuclear membrane protein. Nesprin-3 was the first outer nuclear membrane protein that had a link to the intermediate cytoskeletal system, by binding plectin at the outer nuclear membrane. This was a study by Wilhelmsen et al., 2005, where it was found that expression of Nesprin-3 caused a strong recruitment of endogenous plectin to the outer nuclear membrane and produced colocalization with keratin-6 and -14 filaments. Plectin can bind to Nesprin-3 via its actin-binding domain, leaving the plakin repeats free to associate with the intermediate filament cytoskeleton. Therefore, a link is produced between Nesprin-3a, plectin and intermediate filaments, connecting the nucleus to intermediate filaments (Wilhelmsen et al., 2005). Following this, it was suggested that Nesprin-3a could bind the nucleus to microtubules via MACF1 at the outer nuclear membrane. However, subsequent studies in PA-JEB cells which overexpress GFP-nesprin-3a and -3b proteins with staining for presence of endogenous MACF and microtubules, showed that Nesprin-3a did not have the ability to recruit MACF to the outer nuclear membrane even though microtubules are present at the nuclear envelope. This suggests that unlike the interaction between MACF and Nesprin-3a, the interaction between plectin and Nesprin-3a is specific (Wilhelmsen et al., 2005).

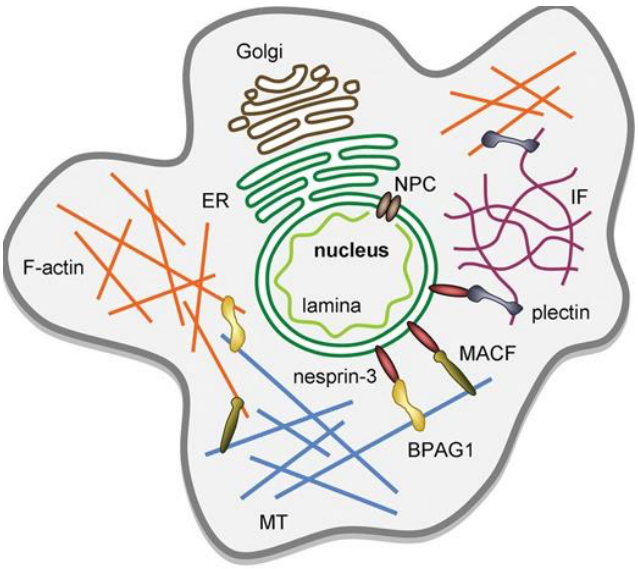

Figure 7 Schematic representation of the interactions of cytolinkers in a cell. Nesprin-3a is able to link the nuclear envelope to IFs or microtubules through its interactions with plectin, BPAG1 and MACF. Plectin can cross-link IFs with F-actin. MACF and BPAG1 can connect the microtubule and actin cytoskeleton. Figure acquired from (Ketema and Sonnenberg, 2011).

Figure 7 created by Ketema and Sonnenberg, (2011) helps to visualise the relationships between the cytoskeletal linkers and the nuclear proteins. Nesprin-3 is one of those proteins that was also included in the experiments of this project.

Research has also revealed that as a spectraplakin protein, MACF1 is associated with with the LINC complex in vitro through binding of its ABD in coimmunoprecipitation to Nesprin-3a (Lu et al., 2012; Wilhelmsen et al., 2005). The result of this binding is not yet fully known. However, our hypothesis is that MACF1 binding to Nesprin-3a may allow Nesprin-3a to link the nucleus to microtubules.

This project began by looking at the properties and functions of MACF1, specifically in its third isoform: MACF1a3, its localisation and distribution in a variety of cell lines. Later, its relationships with cytoskeletal proteins actin and microtubules were studied, followed by cytolinkers nesprin-3 and plectin.

The main aims of this project were:

1. To establish MACF1a3 molecular weight and protein expression level in COS-7, HaCaT, C6 glioma and HDF cells.

2. To examine MACF1a3 distribution and localisation in COS-7, HaCaT, C6 glioma and HDF cells and its relationship with actin and microtubules
3. To check the specificity of the MACF1a3 antibody used via MACF1 silencing experiments
4. To examine nesprin-3 expression level and localisation in the COS-7, HaCaT, C6 glioma and HDF cells
5. To overexpress nesprin-3 and achieve MACF1a3 recruitment to the nuclear envelope
6. To assess whether nesprin-3 is able to recruit plectin to the nuclear envelope
7. To examine ability of mutant nesprin-3 constructs to recruit MACF1a3 and plectin to the nuclear envelope

2. Materials and Methods

Four different cell lines were used as the foundations for carrying out the investigations into the role and interplay of MACF1 iso3 and cytoskeleton features such as Nesprin-3. The protocols for SDS-PAGE, western blotting, transfections and immunofluorescence are outlined below.

2.1 Cell Culture

C6 Glioma, COS-7, HaCat and Human Fibroblast cells were used in the majority of the experiments carried out during this project. All cell lines were maintained in Dulbecco's Modified Eagle's Medium – high glucose (DMEM, Sigma) supplemented with 10% foetal bovine serum (FBS) (Sigma)and 1% Penicillin/Streptomycin (Sigma) at 37 ºC in a 5% CO_2 environment.

Thawing Cells

Vials of the frozen cell lines were originally stored in freezers of -150ºC. Cell thawing was carried out rapidly so as to not allow the Dimethyl Sulfoxide (DMSO, Sigma) in the freezing media to kill the cells. For these cell lines, Dulbecco's Modified Eagle's Medium – high glucose (DMEM, Sigma) supplemented with 10% fetal bovine serum (FBS) from Sigma and 1% Penicillin/Streptomycin (Sigma) was used.

70% ethanol was used to disinfect the cell culture hood and any materials to be placed there. When in the hood, flasks (Greiner Bio-One) and skinny falcon tubes (Starlab) were labelled with the relevant information, such as the cell type, date and passage number. 9ml of warmed DMEM was pipetted (Starlab) into the skinny falcon tube. 1ml of thawed cells were placed into the 9ml of warmed media. Once complete, the frozen cryovial of cells was retrieved from the -150ºC freezer and thawed. Once thawed, contents of the cryovial (Starlab) were removed with a 1ml pipette and placed it into the prepared falcon tube. This was centrifuged for 5 minutes at 1000rpm. Once completed, the supernatant was aspirated, and pellet resuspended in fresh media. The size of the pellet will determine the number of flasks needed. For a large pellet, two flasks may be used initially. For this project, the pellets were generally

resuspended in 10ml of media. 5ml of cell suspension was placed into each flask and topped up to 12ml with fresh media. For a small pellet, one flask may be used. In this instance, resuspend the pellet with 5ml of media and place that into one flask and top up to 12ml with fresh media.

Passaging Cells

When cells reach 70% confluency, they need to be split to keep them viable and healthy. Some cells are immortalised and can be passaged many times whereas others have a limit before they are no longer viable. 1x trypsin (Fisher Scientific) was used to detach the cells from the flask. Cells were passaged in a 1:3 ratio depending on their confluency.

Freezing Cells

Mammalian cells can be frozen down and stored at -150ºC freezers when no longer needed. Cells were frozen down when they had reached a 70-80% confluency. The cell pellet was resuspended in 1ml of ice-cold freezing media (10% DMSO in normal media) (Sigma-Aldrich) per cryovial. The cryovials were placed into the cool cell (Corning, Biocision) and metal ring was inserted into the centre of the cool cell. The cryovials were stored in a -80ºC for one day before being transferred to -150ºC for long term storage.

2.2 SDS-PAGE and Western Blotting

Cell Lysates

To run SDS-PAGE and western blotting experiments, cell lysates are required. For this process, cells must be cultured on 100mm cell culture petri dishes (Greiner Bio-One) to allow for cell scraping and all steps must be completed on ice.

To prepare, Laemmli and RIPA buffers were thawed and kept on ice. The boiler (Eppendorf) was turned on and set to 99 degrees Celsius and the centrifuge to 4ºC

5X Laemmli buffer:

2.5ml of 1M Tris-HCl pH 6.8
4 ml of 10% SDS
2ml of Glycerine
1ml of B-mercaptoethanol
200 microlitres of 10% bromophenol blue
300 microlitres of dH2O.

RIPA buffer:

50mM Tris pH 7.5
150mM NaCl
0.1% SDS
1% Nonidet P-40
0.5% Sodium-deoxycholate
1% Protease Inhibitor

Media from the cells was removed and cells washed twice with sterile PBS and placed on ice. 640µl of RIPA buffer was added and cells scraped off the dish thoroughly with a cell scraper (BD Microlance). Cells were sucked up with a pipette (VWR) into an Eppendorf tube and the tube was incubated on ice for 15 minutes. Using a 25G needle and syringe (BD Microlance), the cells were sheared in the tube 60 times in total. The Eppendorf tube was centrifuged for

10 minutes at speed 13.0 and a temperature of 4ºC. When complete, the supernatant was removed and placed into a clean Eppendorf tube. 160µl of the 5x Laemmli buffer was added and the tube was placed in the Eppendorf boiler at 99ºC for four minutes. The tube was labelled and cooled on ice before being stored in the -20ºC freezer.

SDS PAGE

SDS-PAGE allows for accurate determination of protein molecular weights.

The stock running gel concentration to be used is determined by the predicted protein molecular weight being investigated. Typical concentrations are 3%, 6%, 10%, 12%, 15%, 4%. Recipes for 100ml of varied stock concentration:

3% Resolving Gel

25ml of 1.5M Tris/HCl pH 8.8

10ml of 30% PAA

1ml of 10% SDS

64ml of H2O.

6% Resolving Gel

25ml of 1.5M Tris/HCl pH 8.8

20ml of 30% PAA

1ml of 10% SDS

54ml of H2O.

10% Resolving Gel

25ml of 1.5M Tris/HCl pH 8.8

33.3ml of 30% PAA

1ml of 10% SDS

40.6ml of H2O.

12% Resolving Gel

25ml of 1.5M Tris/HCl pH 8.8

40ml of 30% PAA

1ml of 10% SDS

34ml of H2O.

15% Resolving Gel

25ml of 1.5M Tris/HCl pH 8.8

50ml of 30% PAA

1ml of 10% SDS

24ml of H2O.

4% Stacking Gel

20ml of 0.5M Tris/HCl pH 8.8

13.3ml of 30% PAA

1ml of 10% SDS

65.6ml of H2O.

Stock concentrations were mixed in T75 flasks and stored in the fridge.

Gradient Gels

To visualise higher molecular weight proteins, a gradient gel may be more useful. For the purposes of the experiments within this project, gradient gels of between 3% and 12% were cast.

3% Resolving Gel

25ml of 1.5M Tris/HCl pH 8.8

10ml of 30% PAA

1ml of 10% SDS

64ml of H2O.

12% Resolving Gel

25ml of 1.5M Tris/HCl pH 8.8

40ml of 30% PAA

1ml of 10% SDS

34ml of H2O.

On ice, two falcon tubes were labelled, one for each stock solution. 10% APS and TEMED were defrosted and placed on ice. The gel was cast slowly with the higher concentration of acrylamide at the bottom and lower concentration at the top.

Mix up solutions as follows:

9ml of stock solution (3% and 12%)

30 microlitres of 10% APS

16 microlitres of TEMED

The solutions were mixed up and down and 6ml of each solution was pipetted into the right chambers. The 3% solution goes into the left chamber and 12% into the right. The gradient gel pump is turned on and the thin tube placed in between the glass plates of the gel casting station. The 12% chamber is opened first and allowed to fill to around 1cm before the 3% chamber is opened. When complete, both chambers should be flushed with H2O to prevent polymerisation and blockage within the tubes. Once gel had set, the 4% stacking gel was added.

For non-gradient gels, the running gel can then be prepared in a falcon tube using this recipe:

9ml of desired stock solution

22 microlitres of 10% APS

10 microlitres of TEMED

Once set, remove the butanol and prepare the 4% stacking gel:

3ml of 4% stock solution

30 microlitres of 10% APS

16 microlitres of TEMED

Once set, the glass plates (Bio-Rad) containing the gel were removed from the moulding station and placed into the electrophoresis equipment. SDS running buffer was added to the fill line before the comb was removed.

1 Litre of 10X SDS Running Buffer:

0.25M Tris - 30.25g

2M Glycine - 144g

100ml of 10% SDS

900ml of H_2O.

Once gel has completed running, it can either be used to determine equal loading of lysates using Coomassie staining or for Western Blotting.

Coomassie staining

The gel was removed and placed into a container. Coomassie blue stain was poured over the gel and placed on a shaker for 30 minutes. Once bands were visible, the Coomassie stain was removed and gel lightly washed with water. The gel was viewed over an intelligent light box to examine the loading volumes.

Coomassie Blue Staining Solution:

0.25% Coomassie Brilliant Blue R250 – 2.5g

50% Ethanol – 500ml

10% Acetic acid – 100ml

Make up to 1 litre with H2O.

The solution can also be purchased ready to use from Thermo Scientific.

Western Blotting

To continue with western blotting, prepare the wet-blot buffer needed:

Wet-Blot Buffer – 4 litres

Glycine – 56g

Tris-Base – 12g

40ml of 10% SDS

400ml of 100% Ethanol

Dissolve components in H2O then top up to required volume.

Two litres of wet blot buffer was added to the transfer tank before connecting the transfer tank to the power pack. Transfer was carried out at 10V for 18 hours overnight at 4°C then turned up to 45V for 1 hour and 45 minutes. Once transferred, the membrane was blocked in 5% skimmed milk powder mixed in PBS (Severn Biotech) for 30 minutes. The membrane was rinsed twice with PBS + 0.1% Tween-20 (Sigma-Aldrich) and washed for five minutes on a shaker. The membrane was then incubated with the primary antibody for one

hour on the shaker. Three washes for 5 minutes each with PBS + 0.1% Tween-20 followed before the membrane was incubated with the secondary antibody for one hour on the shaker. The membrane was washed three times for five minutes with PBS + 0.3% Tween-20 followed by three five-minute washes with PBS + 0.1% Tween-20 to reduce background. To visualise the blot, ECL Detection Solution (Bio-Rad) was placed onto the membrane. After one minute, the membrane was removed and placed into the developing box and allowed to develop in the darkroom.

2.3 Cell Transfection

In advance, cells were cultured to an adequate confluency (70-80%). One cuvette and Pasteur pipette per transfection, Nucleofector solution and the relevant plasmids (on ice) were used.

A Nucleofector machine (Lonza) was used to select the relevant cell type. Cells were trypsinized and pellets prepared. The chosen plasmid was added to the wall of the cuvette between the metal plates. Between 3-5µg of plasmid is recommended. The pellet was resuspended in 100µl of Nucleofector solution and added to the cuvette, mixing it with the plasmid. Transfection was carried out using the Nucleofector machine and cells quickly flushed with media and added to 10cm dishes and placed back into the incubator.

2.4 Immunofluorescence

For immunofluorescence experiments, cells are usually grown on 24 well plates (Greiner Bio-One). When they have reached the appropriate confluency, they can be fixed and stained with the appropriate antibodies. An ice box was prepared and PBG and 4% PFA or 4% PFA in 1X BRB-80 was defrosted. Once defrosted, they were kept on ice.

1X BRB-80:

80 mM PIPES

1 mM MgCl2

1 mM EGTA

pH 6.8 with KOH tablets.

PBG:

For 100g:

90 ml of PBS

10ml of 1% fish gelatine stock

1g of BSA

To fix the cells, the media from the wells was removed and cells washed with PBS+0.05% Tween-20 for five minutes. Whilst washing, 10µl drops of 4% PFA or BRB-80 in PFA were placed onto the parafilm (Pechiney). Coverslips (Sigma-Aldrich) were then placed onto the drops. Whilst incubating, the PBS+0.05% Tween-20 in the wells was changed. To permeabilise, coverslips were removed from the parafilm and placed back into the wells and washed for five minutes. Parafilm was changed and 10µl drops of 0.5% Triton X-100 in PBS added. The coverslips were placed back onto the dots and incubated for 10 minutes. The PBS+0.05% Tween-20 in the wells was changed. To block the cells, coverslips were placed back into the wells for five minutes. 10µl drops of PBG were placed onto the parafilm and coverslips placed on top and incubated for 20 minutes.

To stain for antibodies, 10µl drops of primary antibody were pipetted onto the parafilm and coverslips placed on top and incubated for one hour at room temperature. After one hour, the coverslips were washed three time s in PBS + 0.1% Tween-20. Coverslips were then incubated for one hour at room temperature on 10µl drops of secondary antibody. The coverslips were washed three times for ten minutes in PBS + 0.3% Tween-20. 3-5µl drops of mounting media (Vectashield – Vector Laboratories) was added to labelled slides (VWR) depending on the size of the coverslip. The edges were sealed with nail varnish and slides were imaged on Zeiss 880 with Airyscan or AxioVision microscopes at 63x objective lenses.

Tables 1 and 2 below show the primary and secondary antibodies used in the western blotting and immunofluorescence experiments with details of dilutions and manufacturers. Table 3 shows details of the MACF1 siRNA silencing constructs used in silencing experiments, including details of plasmid

sequences of each silencing construct used and manufacturer of the constructs.

Primary Antibody	Species	Dilution	Manufacturer
Anti-Macf1 isoform3	Rabbit	IF: 1:10 WB: 1:250	In-house
Anti-Tubulin WA3	Mouse	IF: 1:100	In-house
Anti-Nesprin-3	Rabbit	IF: 1:50 WB: 1:250	In-house
Anti-Plectin	Mouse	IF: 1:200	Santa Cruz Biotechnology
Anti-β actin	Mouse	WB: 1:5000	Sigma-Aldrich
Anti-myc	Mouse	1:1	Abcam

Table 1 Primary antibodies used in Immunofluorescence (IF) and Western Blotting (WB). Details of the primary antibodies used, species antibodies were raised in and dilutions used in immunofluorescence and western blotting experiments.

Secondary Antibody	Species	Dilution	Manufacturer
TRITC-Phalloidin	-	IF: 1:200	Sigma-Aldrich
Chicken Alexa Fluor 488	Anti-Rabbit	1:1000	ThermoFisher
Goat Alexa Fluor 568	Anti-Mouse	1:1000	ThermoFisher
DAPI	-	1:1000	ThermoFisher

Table 2 Secondary antibodies used in Immunofluorescence (IF). Details of the secondary antibodies used in immunofluorescence experiments, species they were raised in and dilutions used.

Plasmid/Construct	Plasmid Sequence (5' to 3')	Manufacturer
MACF1iso3 siRNA #1	CTCCCATATCTCCTAAGAAGAAGCTTGTTCTTAGGAGA TATGGGAGTTTTTT GATCAAAAAACTCCCATATCTCCTAAGAACAAGCTTCT TCTTAGGAGATATGGGAGCG	Invitrogen
MACF1iso3 siRNA #2	ATTGCTCACCTGCTTGATAAGAAGCTTGTTATCAAGCA GGTGAGCAATTTTTT GATCAAAAAATTGCTCACCTGCTTGATAACAAGCTTCT TATCAAGCAGGTGAGCAATCG	
MACF1iso3 siRNA #3	GCCAACTGGTGGAATTTCCGAAGCTTGGGAAATTCCAC CAGTTGGCTTTTTT GATCAAAAAAGCCAACTGGTGGAATTTCCCAAGCTTCG GAAATTCCACCAGTTGGCCG	

Table 3 MACF1 siRNA silencing constructs used in silencing experiments. Details of plasmid sequences of each silencing construct used and manufacturer (Invitrogen) of the constructs.

3. Results

3.1 Analysis of MACF1a3 structure using bioinformatics

Uniprot is a scientific database which provides a comprehensive resource for protein sequences and functional information. This website was used to begin carrying out bioinformatics studies and it shows protein sequences for 4 of the 7 isoforms: MACF1b and isoforms 2, 3 and 5 of MACF1a. As the focus of this project was MACF1a3, I firstly compared this isoform with MACF1b, which the website considers as the canonical sequence with which all the other sequences produced refer to. This isoform is also known as MACF1b on the website. The data discussed here relates to the data available on the website.

MACF1b is the largest of all four isoforms at 838kDa and with protein sequence length of 7388 amino acids. Contrastingly, MACF1a3 has a mass of approximately 614kDa and a protein sequence length of 5374. Analysing and aligning the two sequences has shown that there are changes in the protein sequences as well as sections missing between the two isoforms. The first change that is clear to see is that there are sequence changes from residue 1 to 72 between MACF1b and Macf1a3. This sequence at the beginning of both isoforms, although different, still confers calponin homology domains (CH). CH domains are protein modules made up of approximately 100 residues and were first identified at the N-terminus of calponin, which is an actin-binding protein (Korenbaum, 2002). The CH domain has an α-helical fold structure and as it is an actin-binding protein, it is required for stability and organisation of the actin cytoskeleton and activation of various downstream pathways. In the spectrin family of proteins, there are usually two CH domains found working together in tandem: CH1 and CH2. The CH1 domain has an intrinsic ability to bind F-actin whilst CH2 when it binds in tandem with CH1 is required to facilitate high-affinity binding of F-actin.

When this protein sequence was entered into the website SMART (Simple Modular Architecture Research Tool), it produced a schematic diagram of the structure of MACF1a3 and its domains, recreated and presented in Figure 8. However, one feature which is not shown is MACF1a3's unique longer N-

terminus with a unique 5' untranslated region (UTR). The MACF1a3 antibody used in this project binds to the unique, longer N-terminal sequence of the MACF1a3 protein.

The 5' UTR region is a region of mRNA which is upstream from the initiation codon and has roles in regulating translation of transcripts using various mechanisms.

Spectrin repeats are present in all members of the spectrin family and its residues are folded into α-helices. These helices are then formed into anti-parallel coiled coil repeats which then act as spacer regions, separating different domains at the N-terminus and C-terminus as well as allowing the protein to have flexibility to move. All MACF1 proteins also contain two EF-hand motifs at the C-terminus which is conserved to the spectrin family. The EF-hand motifs are involved in intracellular calcium binding and are essential for cellular processes as calcium ions are considered to be secondary messengers involved in intracellular and extracellular signalling (Denessiouk et al., 2014). After the EF-hand motifs, there is a GAS2-related protein (GAR) domain which is specific and unique to spectraplakins. This domain's function is to bind and stabilise microtubules and is found at the C-terminus of the protein (Hu et al., 2016).

Aside from sequence changes, the alignment tool on BLAST shows that there are regions missing in MACF1a3 which are present in MACF1b. These missing proteins are in the sequence region of 1543-3609 where the plectin repeats are located and 4410-4430. Although the website refers to these domains as plectin domains, Hu et al 2016 have described them as plakin domains and plakin repeat domains. They also add that this plakin repeat domain is unique to the MACF1b isoform, which is confirmed by the sequence alignment carried out above showing that this plakin repeat domain is not present in MACF1a3. This deletion can also account for the reduced mass of MACF1a3 in comparison to MACF1b.

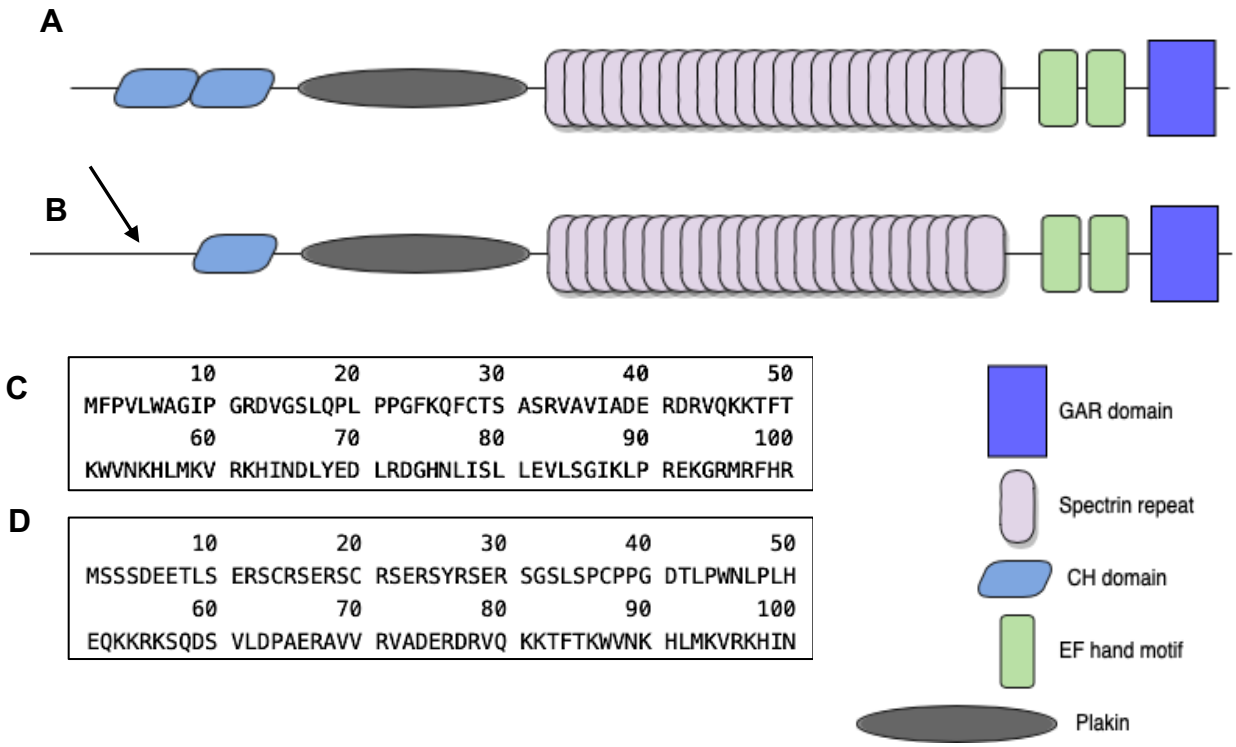

Figure 8 Diagram showing the domain architecture of MACF1b (A) and MACF1a3 (B). Protein sequence analysis shows the sequence difference in MACF1b (C) and MACF1a3 (D). Arrow points to chosen epitope of MACF1a3 to which the antibody anti-MACF1a3 binds. A) Domain structure of MACF1b shown with complete CH domains, plakin domain, 23 spectrin repeats, EF hand motif and GAR domain. B) Longer N-terminus and presence of only CH2 domain shown. C and D) The starting sequences of MACF1b and MACF1a3 are not identical, relating back to A and B, showing different domain structures and organisation.

3.2 Establishment of MACF1a3 molecular weight and expression level in COS-7, HaCaT, C6 and HDF cells

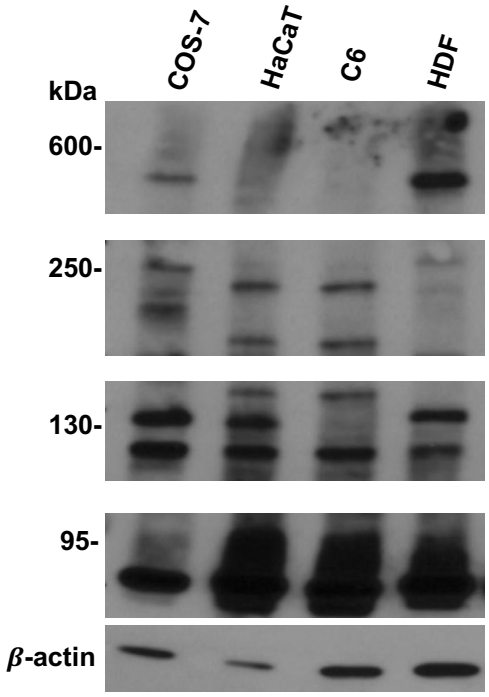

Figure 9 Western blot analysis of MACF1a3 molecular weight and expression level in cell lines. Blot produced by a 3-12% gradient gel showing expression levels of MACF1a3 in COS-7, HaCaT, C6 and HDF cells. Protein from lysates was transferred overnight at 10V for 18 hours and turned up to 45V for 1 hour and 45 minutes. Blocking was done in 5% milk. Loading control used was β-actin. The bands show varying levels of expression of MACF1a3 in the different cell lines. Multiple bands at different molecular weights are seen.

These cells were cultured in their wildtype form to allow determination of MACF1a3 protein expression in each and to test whether the antibody used was specific by checking the molecular weight of bands expressed.

The MACF1a3 antibody is expected to detect the MACF1a3 protein at a predicted molecular weight of 600 kDa. The bands shown in Figure 9 all come from one continuous gel which has been split up into the panels shown for improved visualisation. There are bands which are expressed at 600 kDa, indicating that the MACF1a3 antibody is in fact specific. There is also some expression above the 600 kDa mark. This expression could be explained as being non-specific or it may be that there was a problem with the gradient gel used as it may have been allowed to run for longer than necessary. If this experiment were to be repeated, it may be necessary to further check the

specificity of the antibody and to pay closer attention to the types of gels which may be used. For example, an experiment into running the gradient gels for various lengths of time may be beneficial to establish exactly the right time needed to find detection of the protein at the expected mass. Figure 9 shows that there were several bands detected which varied in molecular weight. There were two distinct bands detected at the 600 kDa mark in COS-7 and HDF cells which can be detected faintly in HaCaT and not observed in C6 cells. Furthermore, there were two bands expressed at 250 kDa in COS-7, HaCaT and C6 cells which were stronger in expression than the weak bands seen in HDF cells. At the 130 kDa mark, there are two bands expressed in all the cell lines apart from in C6 cells. Further down at the 95 kDa mark, there was stronger expression detected in all cell lines aside from COS-7, in which one clear band can be observed. The blot showed that there was strong expression of MACF1a3 in all the cell lines, albeit at different molecular weights. However, at 600 kDa, the strongest expressors were COS-7 and HDF cells as there are distinct bands detected in those cell lines when compared with HaCaT and C6 cells.

3.3 Examining distribution and localisation of MACF1a3 in cell lines alongside actin filaments

As MACF1 is a spectraplakin protein, it has the ability to bind both actin filaments and microtubules. Therefore, the logical next step was to carry out immunofluorescence investigations into the localisation of MACF1a3 in each of the cells used in this experiment in correlation with actin and microtubules and visualise the staining patterns of the three in each cell.

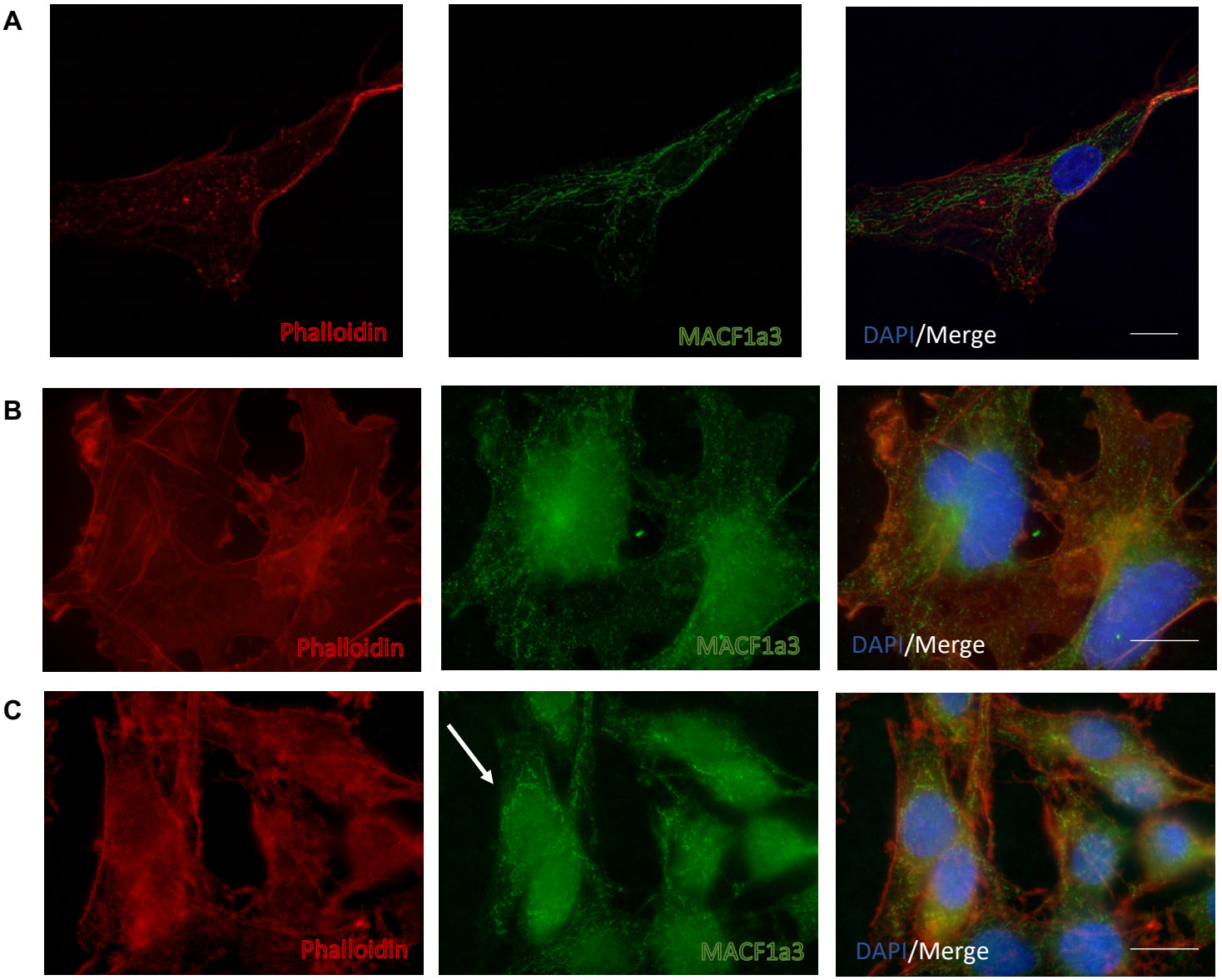

D

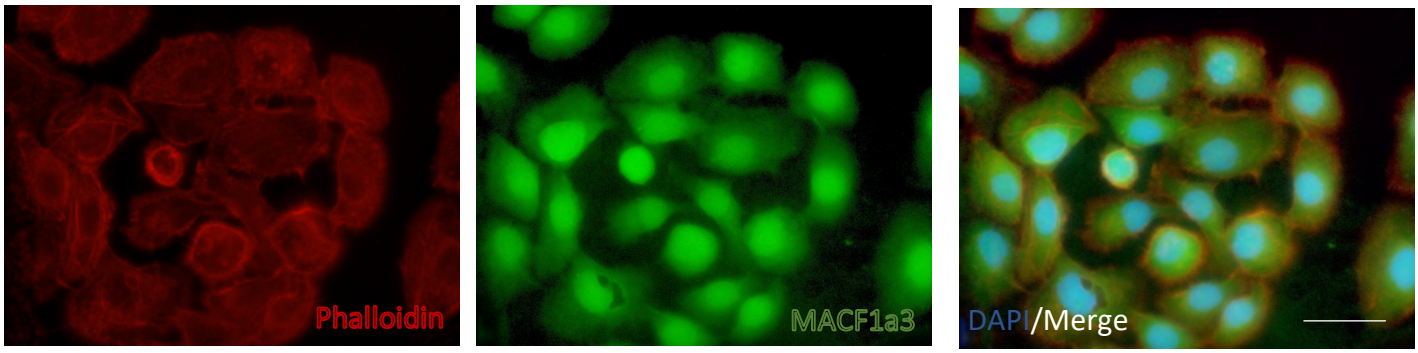

Figure 10 Images showing distribution of MACF1a3 in A) HDF cells B) COS-7 cells C) C6 glioma cells D) HaCaT cells with TRITC-labelled Phalloidin staining to detect F-actin filaments. Cells were cultured to 70% confluency before being fixed in 4% PFA and stained, using immunofluorescence protocol described in methods section, with MACF1a3 and TRITC-Phalloidin to examine distribution of MACF1a3 in each cell line and its relationship with actin filaments. A) Imaged with confocal microscopy using Zeiss 880. B), C) and D) Imaged with Axiovision microscope. Arrow in Figure 10C points to an example of nuclear envelope staining in C6 cells. Scale bars 25μm

MACF1a3 presents differently in each cell line and a pattern of distribution which was equal in all could not be found. For example, in HDF cells, MACF1a3 appeared to be filamentous, producing long, track-like staining throughout the cell. In contrast, staining of MACF1a3 in COS-7 cells appeared 'dotty' throughout the cytoplasm and did not show the same long, filamentous structures previously seen in HDF cells. For HaCaTs, it was consistently difficult to produce staining of MACF1a3 which was similar to the filamentous and cytoplasmic staining seen in COS-7 and HDF cells. However, there was prominent nuclear staining observed in HaCaTs. As is presented in Figure 10D, clear structures or staining patterns were not easy to see and it was difficult to reach any conclusions with regards to how MACF1a3 distributes itself throughout HaCaT cells from this stain.

C6 cells are shown in Figure 10C. The staining here was also faint, but it was possible to see that MACF1a3 was organised in grainy or 'dotty' cytoplasmic structures. Furthermore, it showed that there was some staining around the nuclear perimeter, highlighted using the arrow on Figure 10C. It was not however, distributed all the way around the nucleus and thus was difficult to state that the staining is around the nuclear envelope represented a clear nuclear envelope ring.

From Figure 10C, some staining close to the nucleus can be seen. To further investigate whether there was staining around the nuclear envelope in C6 cells, 300 cells from the same experiment in Figure 10C were counted and quantified. The data plotted on the graph was collected when examining C6 cells stained for MACF1 staining around the nuclear envelope. The arrow in Figure 10C points to an example of the types of cells with stronger staining around the nuclear envelope that were plotted as a positive result.

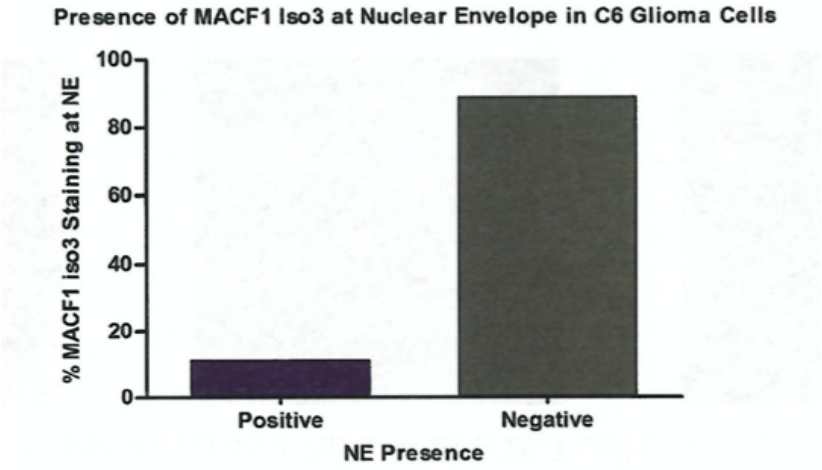

Figure 11 Quantification of MACF1a3 presence at nuclear envelope of C6 glioma cells. 300 cells were counted, and results plotted were based on whether nuclear envelope staining could be seen or not. MACF1a3 nuclear envelope staining was observed in approximately 10% of cells counted.

Figure 11 shows that clear nuclear envelope rings were found in only 10% of the C6 glioma cells and in the majority of the C6 cells, MACF1a3 was found to be in the nucleus, shown by the nuclear staining in Figure 10C.

3.4 Examining distribution and localisation of MACF1a3 in cell lines alongside microtubules

The images below in Figure 12 show COS-7, HaCaT, C6 and HDF cells stained with a mouse anti-tubulin WA3 antibody and fixed with 4% PFA in 1x BRB-80 at an ice-cold temperature to investigate the relationship between Macf1a3 and microtubules in cells.

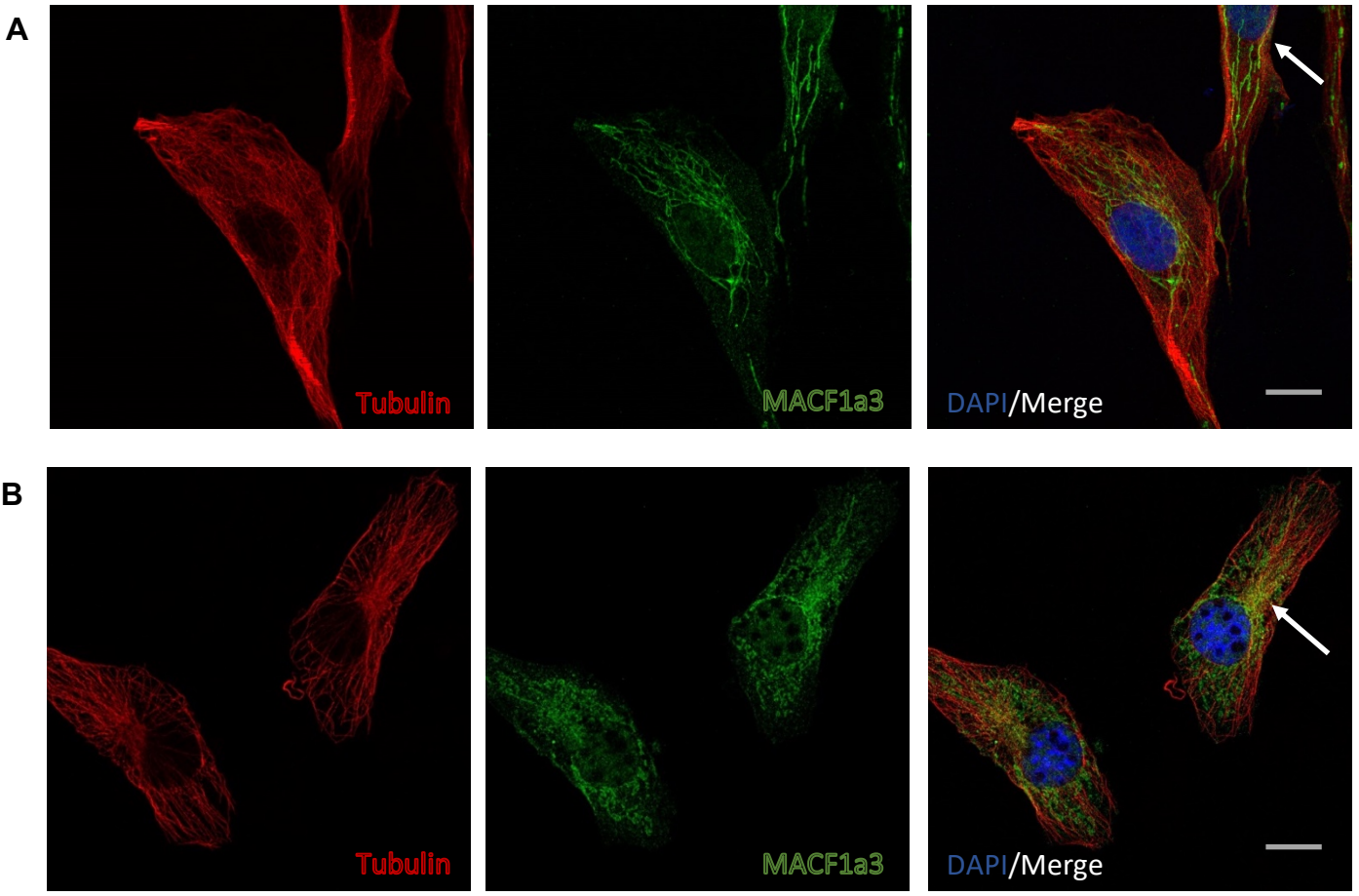

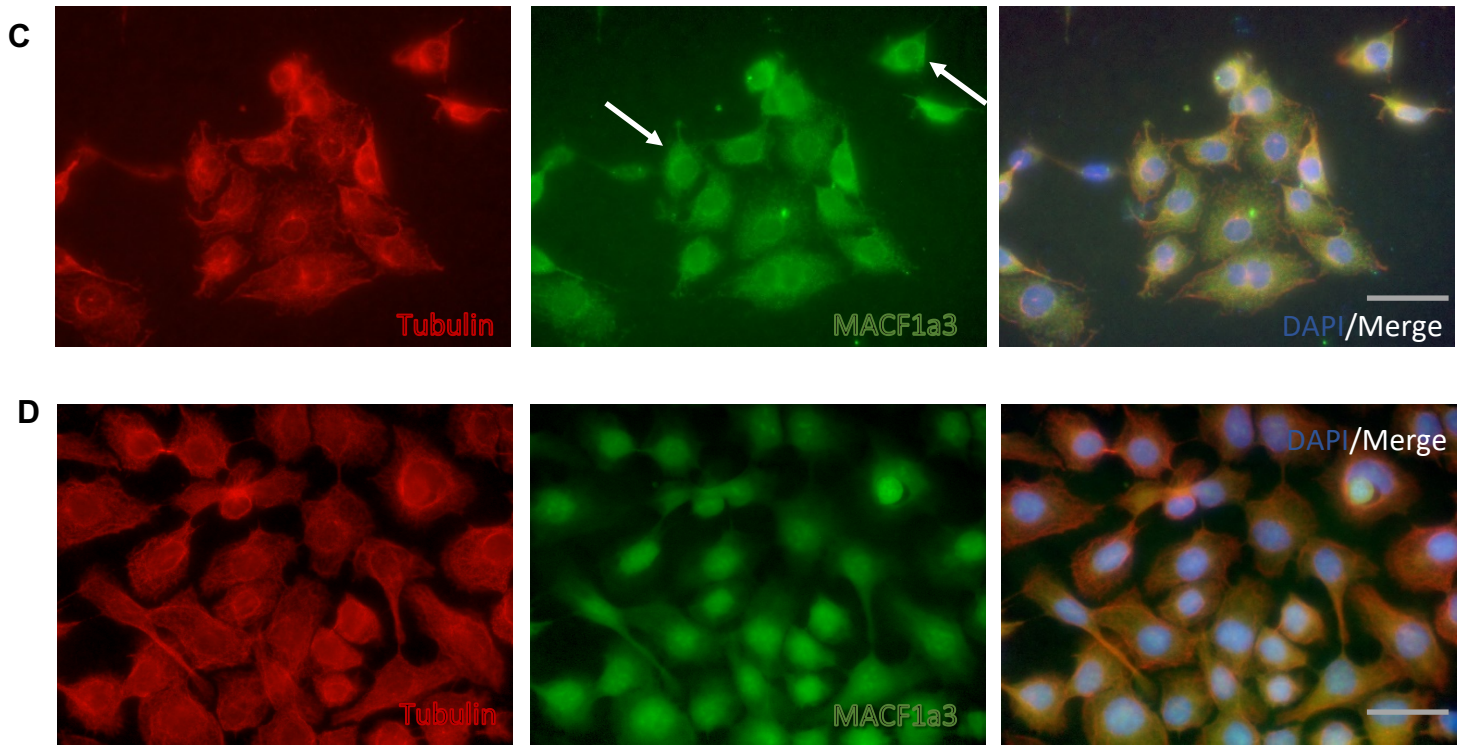

Figure 12 Images showing distribution of MACF1a3 in A) HDF cells B) COS-7 cells C) C6 glioma cells D) HaCaT cells with anti-tubulin WA3 antibody to stain for microtubules. Cells were cultured to 70% confluency before being fixed in 4% PFA and stained, using immunofluorescence protocol described in methods section, with MACF1a3 and anti-tubulin WA3 antibody to examine distribution of MACF1a3 in each cell line and its relationship with microtubules. A) and B) Imaged with Zeiss 880 microscope. C) and D) Imaged with Axiovision microscope. Scale bars 25μm

It was difficult to initially find the correct concentration of anti-tubulin antibody required to get a signal to be able to assess the relationship between MAC1a3 and microtubules. This was achieved through trial and error and gradually increasing the concentration of the antibody in PBG. The images in Figure 12 show that MACF1a3 follows the same distribution pattern within each cell when stained with anti-tubulin as it did with phalloidin. The arrows in Figure 12C show that these C6 cells seemed to have more prominent staining around the nuclear envelope than those in Figure 10C. Moreover, this figure is a good example of the type of staining around the nuclear envelope in C6 cells that were used in Figure 11. As in the immunofluorescence experiments with phalloidin, HaCaT cells shown in Figure 12D showed similar prominent nuclear staining as in Figure 10D but it was again difficult to see any filamentous or clear cytoplasmic structures as was observed in COS-7 and HDF cells. Initially, COS-7, HaCaT, C6 and HDF cells were being fixed with 4% PFA in ice-cold 1x BRB-80. It was suggested that the

reason the tubulin antibody was not working to stain microtubule filaments was due to the BRB-80 used to fix the cells being ice-cold rather than at room temperature. Therefore, a short experiment was carried out using a new anti-tubulin antibody (anti-tubulin WA3).

3.5 Examining staining efficiency of microtubule filaments in COS-7 and HDF cells against temperature and different antibody type

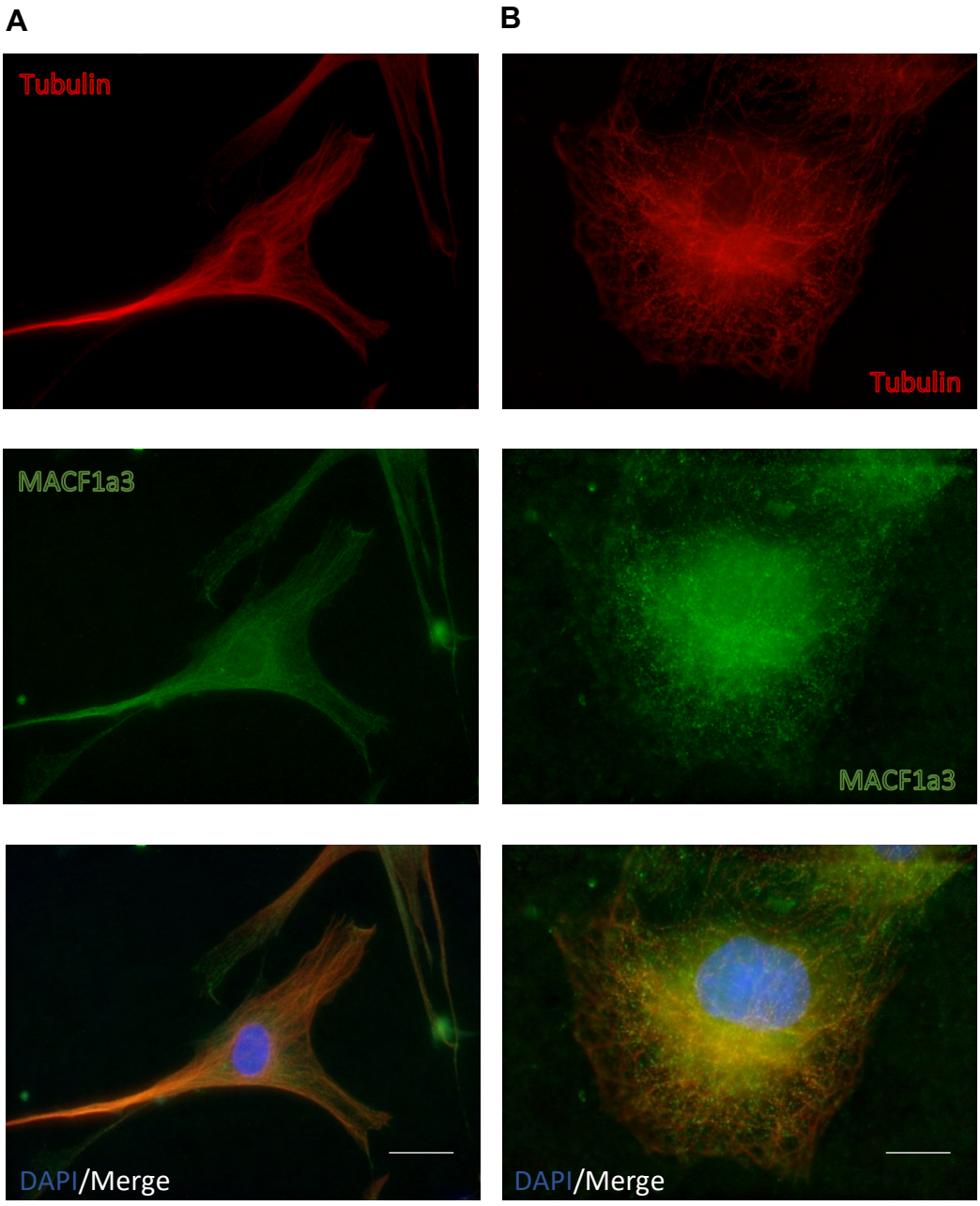

Figure 13 Images showing microtubule and MACF1a3 structure in A) HDF cells and B) COS-7 cells following fixation with 4% PFA in ice-cold 1x BRB-80. Microtubule structure is undisturbed following fixation with ice-cold BRB-80. MACF1a3 structure is the same as was described for Figure 10 and 13. A) and B) Imaged with Zeiss 880 microscope. Scale bars 25μm

This short experiment was carried out as it was suggested that a reason for the consistent lack of microtubule staining could be due to the fact that ice cold BRB-80 was being used to fix the cells. The hypothesis was that the temperature of the BRB-80 was causing the microtubule filaments to be destabilised and hence produce no staining. This staining was carried out using the dilutions specified in Table 1 and cells fixed with ice-cold BRB-80. A new anti-tubulin antibody was also used, in the form of anti-tubulin WA3. This experiment showed that the lack of microtubule staining was not due to the temperature of BRB-80 used to fix the cells but rather the type of primary anti-tubulin antibody used was not producing a signal. The images in Figure 13 prove that the microtubule networks in HF and COS-7 cells are intact despite the fact that it was suggested that ice-cold BRB-80 may be the reason why no tubulin staining was being produced.

3.6 MACF1a3 silencing construct #2 produced a partial knockdown effect

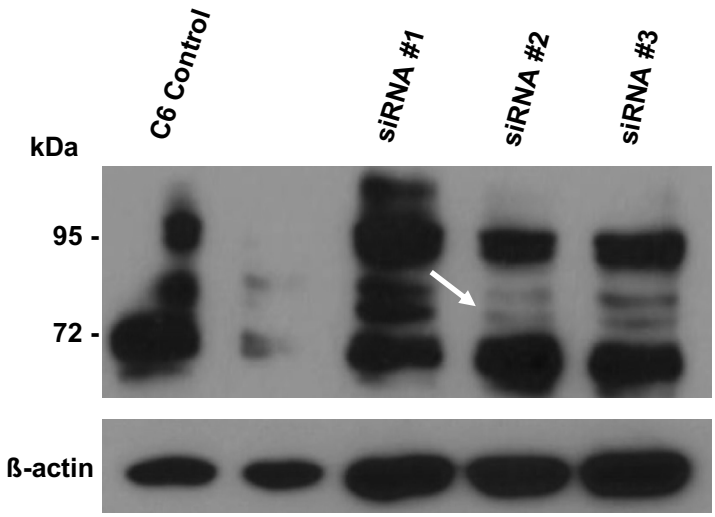

Figure 14 Examining effect of MACF1a3 silencing in C6 glioma cells using three siRNA constructs. Three MACF1a3 silencing constructs were transfected into C6 glioma cells and lysates produced run on 6% gel with a control C6 lysate. Lysates were run through a gel at 120V and transferred at 128mA. A β-actin control was used to assess equal loading volumes. Arrow points to siRNA #2 which showed the greatest knockdown when compared to siRNA #1 and #3. (Lane 2 contains a repeat C6 control lysate which did not transfer correctly but was not removed from the western blot image).

Three silencing constructs were produced by Invitrogen with the sequences provided in Table 3. The siRNA constructs are each targeted at a different sequence location and were transfected into C6 glioma cells.

A control was used in the form of a wildtype C6 cell lysate. This was to test the expression and knockout effect of the Macf1a3 silenced constructs compared to the Macf1a3 expression in a wildtype cell. This experiment was carried out initially to test the specificity of the MACF1a3 antibody and is an experiment which can be used and developed further to work with silencing and knockout studies. Western blot analysis from this experiment showed that a full knockdown was not achieved. Although it was clear to see that full silencing was not achieved, the blot did show that construct #2 produced the greatest knockdown effect when compared to the construct #1 and #3, highlighted by the arrow in Figure 14. This was a promising start and

demonstrated that at least one of the constructs could be used in the future for further studies into silencing. Some improvements on this experiment may be to use C6 cells which are newer and have been passaged less than the ones used in this project, taking greater care at the transfection stage to ensure minimal cell death from the transfection process and possibly to incubate the cells for a longer period of time to allow them to grow and recover from the transfection process. These suggestions may be of use to future studies to examine whether construct #2 can indeed achieve a full knockdown effect of MACF1a3.

3.7 Investigating the relationship between MACF1a3 and mitochondria

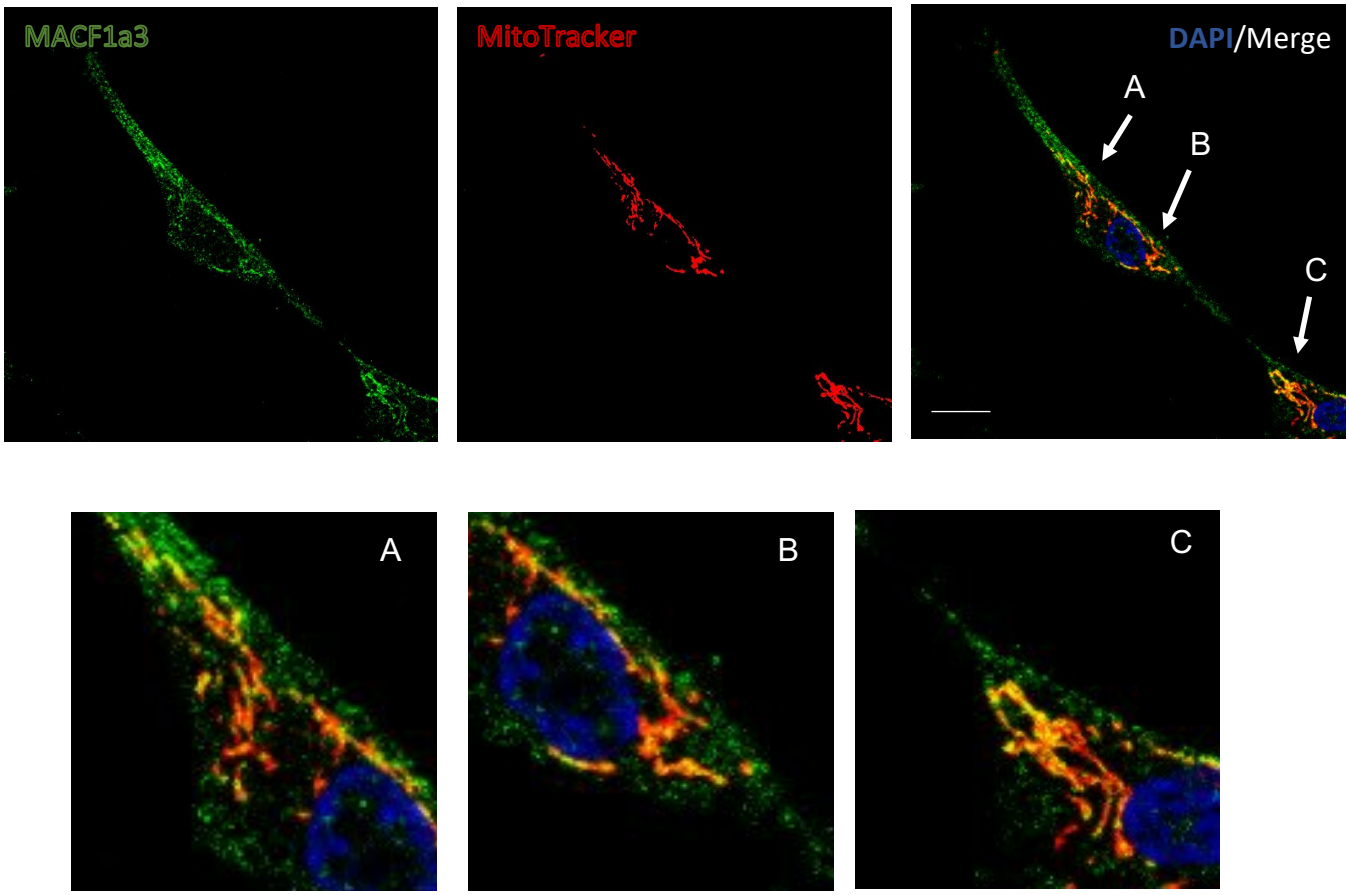

Figure 15 Images showing MACF1a3 staining alongside mitochondrial staining. HDF cells were stained with MitoTracker, added to DMEM media at a dilution of 1:10000 and incubated for 15 minutes before being fixed with 4% PFA and stained with anti-MACF1a3 antibody. Arrows point to areas of possible colocalization, with corresponding panels showing enlarged images of the three regions labelled A, B and C. Cells were imaged on Zeiss 880 confocal microscope and arrows point to potential sites of colocalization. - Scale bars 25µm

From studies carried out by Ghasemizadeh et al. in 2019, it was shown that MACF1 has an effect on mitochondria positioning and organisation and that Macf1-KO mice show decreased muscle excitability and high mitochondria content. From this, it is clear that MACF1 is either directly or indirectly working with mitochondria within cells. An interesting hypothesis therefore was that MACF1a3 could be colocalising with mitochondria in cells and thus was briefly investigated. HDF cells were used for this experiment due to their strong expression of MACF1a3, shown in Figure 9, and also as they have strong filamentous and

cytoplasmic staining for MACF1a3 in immunofluorescence studies, as shown in Figures 10 and 12. From Figure 15 and the arrows shown, it is possible that there is some colocalization occurring between Macf1a3 and mitochondria in the HDF cell. However, this requires more experimental work which was not possible to be carried during this project. Further imaging for colocalization studies is required. This can be carried out with the Zeiss 880 microscope to create Z stacks or imaged further using super resolution microscopy, followed by quantification of the level of colocalization between the two components if present using ImageJ software.

3.8 Examining nesprin-3 domain structure, molecular weight and expression levels in COS-7, HaCaT, C6 and HDF cells.

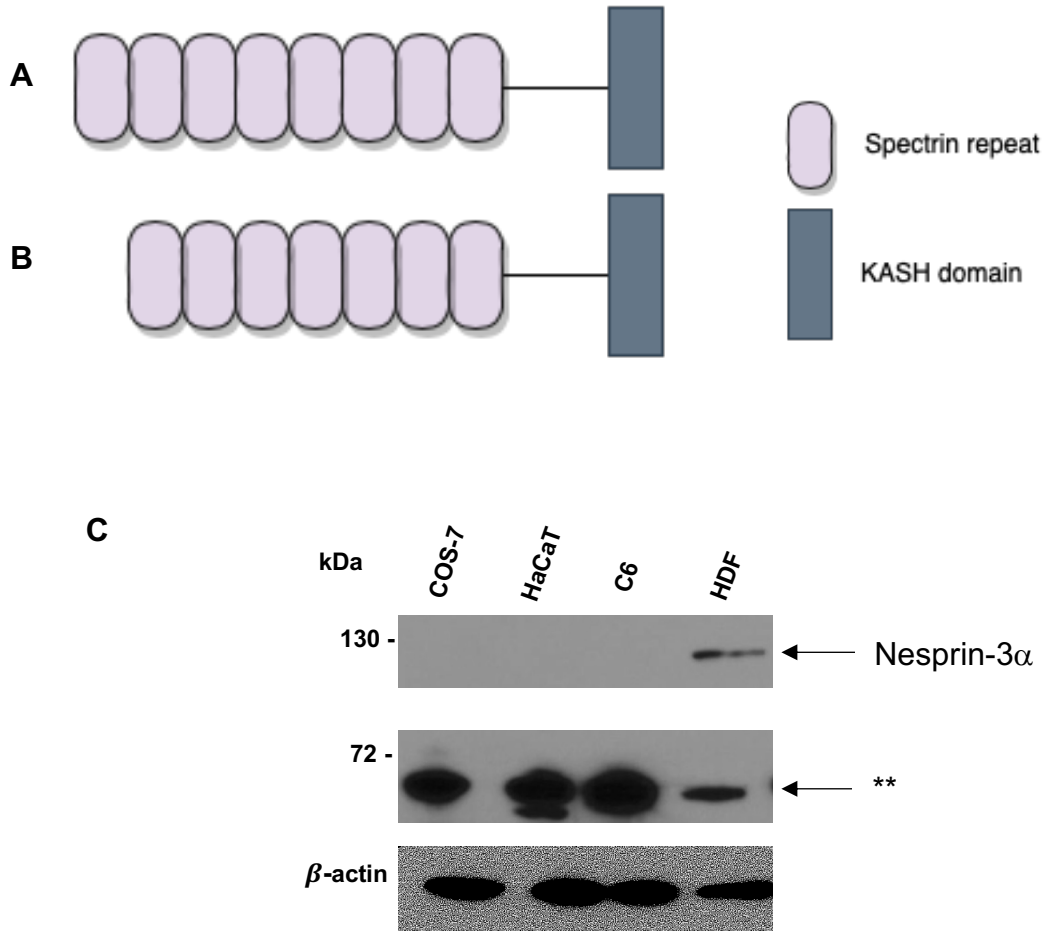

Figure 16 Schematic diagram of the domain structure of nesprin-3 in a mouse and western blot analysis of nesprin-3 expression and protein level in COS-7, HaCaT, C6 and HDF cells. A) Nesprin-3a and B) Nesprin-3ß showing presence of 8 and 7 spectrin repeats respectively. C) COS-7, HaCaT, C6 and HDF lysates run on 6% gel and transferred at 128mA for 1 hour and 20 minutes. A rabbit anti-nesprin-3 antibody was used at a dilution of 1:250. β-actin control was used to check for equal loading volumes. Western blot of nesprin-3 expression shows strongest expression at higher molecular weight around the 130kDa mark in HDF cells only and at lower molecular weight of around 72kDa in C6 cells. ** - non-specific bands detected below 72 kDa

The protein sequences and functional information of nesprin-3 was found on the Uniprot database. Searching for nesprin-3 shows its protein sequence in many organisms from humans and mice to zebrafish. Interestingly, according to the website, human nesprin-3 has

three different isoforms whereas mouse nesprin-3 has two. The isoforms are a product of alternative mRNA splicing. The human nesprin-3 isoforms 1,2 and 3 have masses of approximately 112kDa, 111kDa and 69kDa respectively. The isoforms of mouse nesprin-3 (1 and 2) have masses of approximately 112kDa and 102kDa respectively. The diagram produced in Figure 16A shows isoforms 1 and 2 (nesprin-3α and nesprin-3β) of nesprin-3 in mice. Nesprin-3α contains 8 spectrin repeats whereas nesprin-3β has only 7, as shown in Figure 16A and B.

From the blot, it is clear to see that nesprin-3 is expressed in all the cell lines at the lower molecular weight of approximately 69kDa, with a doublet seen in HaCat cells (highlighted with an arrow). The strongest expression at this weight was in C6 cells. Although there was nesprin-3 expression in all four cell lines at the lower molecular weight, there was only expression of full-length nesprin-3 in HDF cells at approximately 115kDa. However, the bands detected below 72 kDa may in fact be non-specific.

3.8.1 Visualising nesprin-3 expression in COS-7, HaCaT, C6 and HDF cells

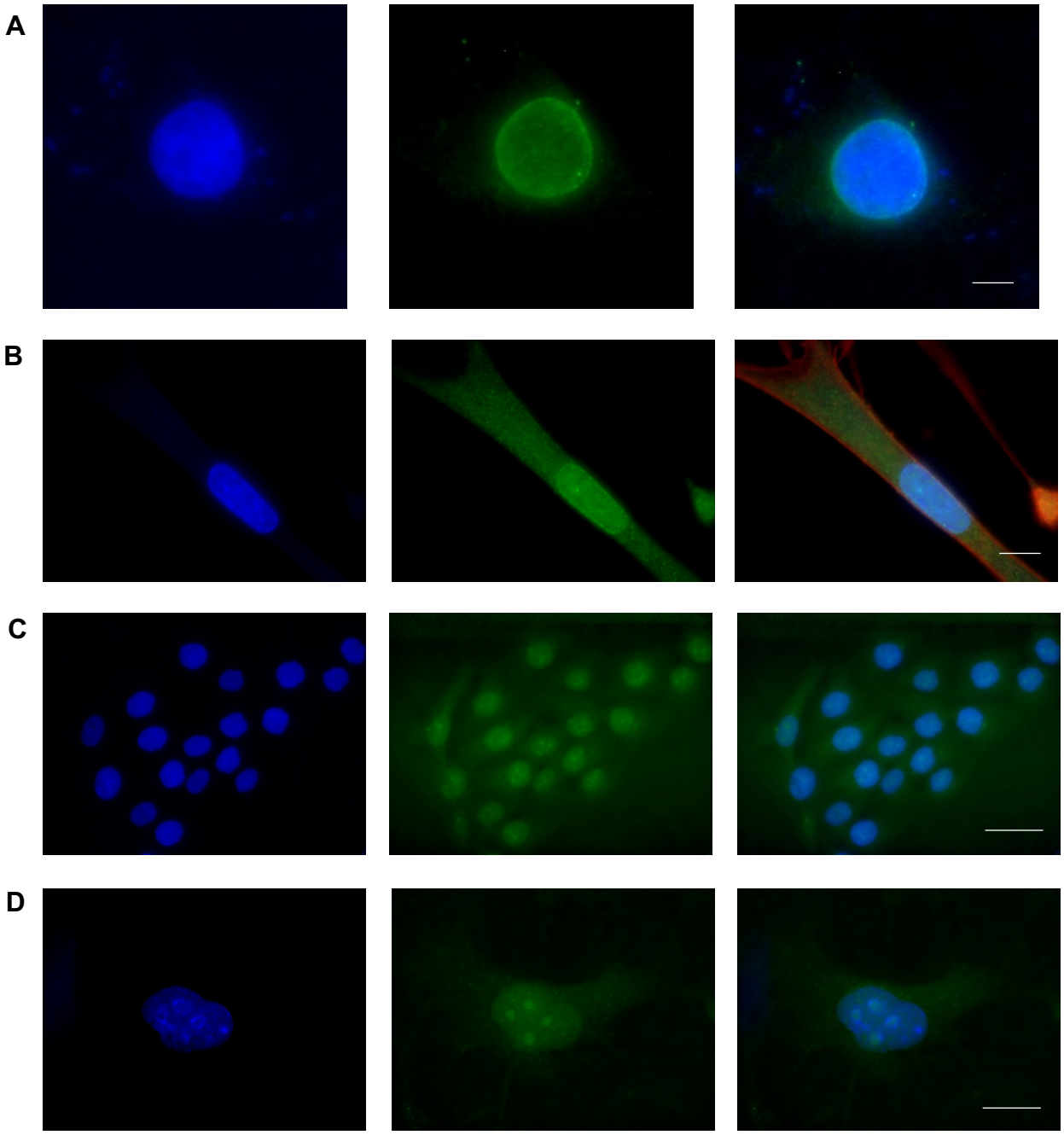

Figure 17 Images showing the localisation of Nesprin-3 in A) C6 cells B) HDF cells C) HaCaT cells and D) COS-7 cells. Cells were cultured to 70% confluency before fixation with 4% PFA and staining with anti-nesprin-3 antibody. Nuclear envelope rings were observed in C6 and HDF cells. Staining was too weak in COS-7 and HaCaT cells to assess presence of nesprin-3 at the nuclear envelope. All cells imaged with Axiovision microscope. Scale bars: 25μm

C6 and HDF cells produced a stain which was both around and through the nucleus and generally produced a clearer staining pattern. HDF

cells were also stained through the cytoplasm as shown in Figure 17B, which could be non-specific background staining.

The staining in COS-7 and HaCaT cells however was not specific to the nuclear envelope and appears to be cytoplasmic and through the nucleus. It was difficult to obtain a strong signal in COS-7 and HaCaT cells and there appears to be a large amount of background staining which is non-specific to the structures in the cell. The western blot analysis of nesprin-3 in the cell lines may offer an explanation for this. Although the higher molecular weight band was only expressed in HDF cells, the strongest signal from the lower molecular weight band around the 69kDa mark was in C6 cells and COS-7 and HaCaT cells had the weakest expression of nesprin-3. Therefore, a reason for the lack of specific staining may be that COS-7 and HaCaT cells do not express nesprin-3 at a level great enough to produce high quality staining around the nuclear envelope. Another reason may be that the anti-nesprin-3 antibody was not used at the right concentration and may need to be more concentrated to produce a signal. However, this can also create a problem of more background staining and thus further work to test this suggestion is required.

3.9 Overexpression of WT nesprin-3α in COS-7 does not promote recruitment of MACF1a3 to the nuclear envelope

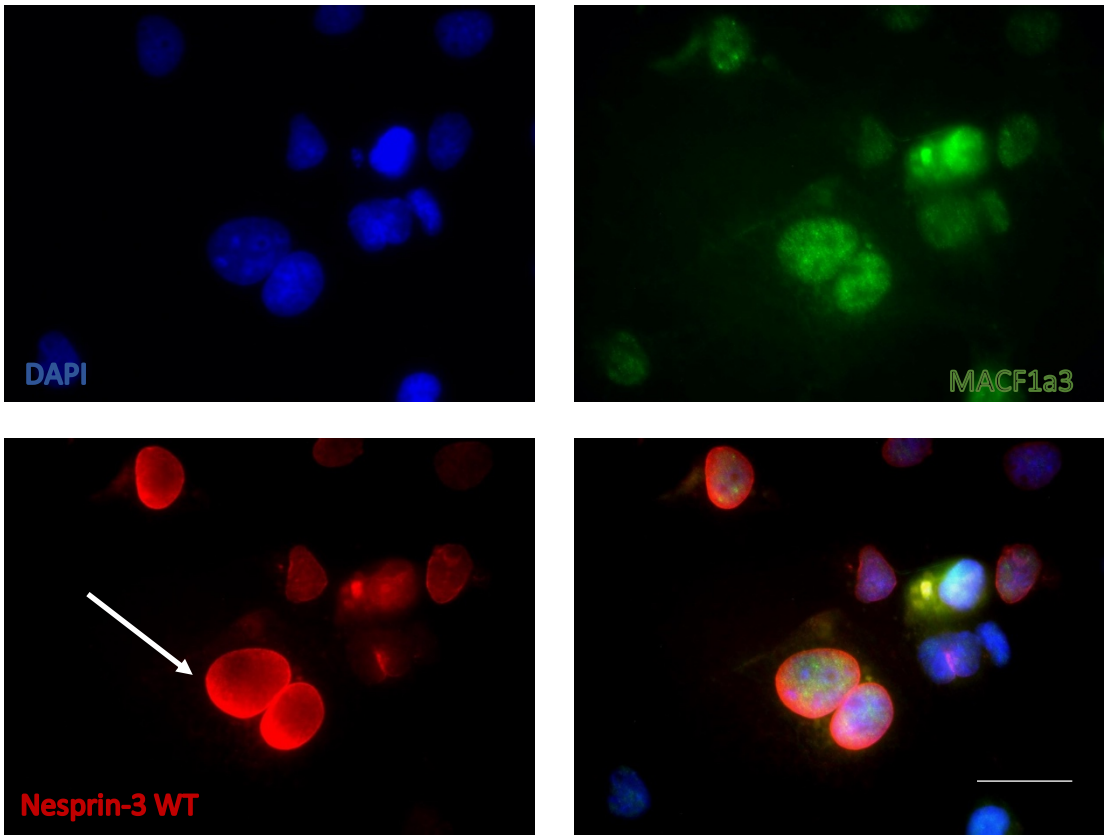

Figure 18 Transfection of COS-7 cells with nesprin-3 WT to assess MACF1a3 recruitment to nuclear envelope. COS-7 cells were transfected with myc-tagged wildtype nesprin-3α plasmid. Cells grown and fixed and imaged on Zeiss Axiovision microscope. Transfected COS-7 cells overexpressing WT nesprin-3α could not recruit MACF1a3 to the nuclear envelope. Scale bars: 25μm

COS-7 cells were transfected to overexpress nesprin-3 with a myc-tagged wildtype nesprin-3 plasmid. The hypothesis for this experiment was that an overexpression of nesprin-3 would result in Macf1a3 recruitment to the nuclear envelope. The cells were grown to a 70% confluency on coverslips before being fixed. 300 transfected cells such as the ones highlighted in Figure 18 by the arrow were counted to check for recruitment of Macf1a3 to the nuclear envelope. This transfection showed no recruitment of Macf1a3 to the nuclear envelope. An improvement to this investigation for future experiments would be to provide western blot data showing the levels of overexpression of the myc-tagged nesprin-3 to verify that it does have the expected size and

use this data as an additional control experiment. However, from this study and the overexpression of nesprin-3 in this project, it is clear that MACF1 may not have the strong binding affinity needed to interact with and be recruited by nesprin-3 as there may be other cytolinkers such as plectin for example, which hold greater and more specific interaction abilities. This relationship between MACF1, nesprin-3 and plectin encouraged the start of the final set of experiments carried out in this project.

3.10 Nesprin-3 sequence analysis: H222Y and A927E

The next and final set of experiments involved two forms of nesprin-3 constructs: nesprin-3 WT, and a mutant form of nesprin 3, H222Y and A927E. They were used to analyse differences in their ability to recruit MACF1a3 and plectin to the nuclear envelope. H222Y and A927E are mutations in the nesprin-3 protein. H222Y is an amino acid change from histidine to tyrosine at position 222 and are both polar amino acids whereas A927E is an amino acid change from alanine to glutamic acid. These are examples of missense mutations. Missense mutations occur when there is a single base substitution at the DNA level, causing the codon to code for a different amino acid at the protein level. If this change results in a new amino acid which has similar properties to the original, it is called a conservative change. If the mutation leads to a loss in the protein's function and results in disease, it is referred to as non-conservative.

The constructs were received as part of a collaboration with Oxford University. All three constructs were myc-tagged. The constructs received from the patient possessed compound heterozygous mutation for H222Y and A927E. Compound heterozygosity in genetics is when one individual has two or more heterogenous recessive alleles for the same gene. Both alleles may be mutated but at different locations within the gene, which is what was provided in these constructs. The phenotype this mutation displays is cerebellar ataxia, intellectual disabilities, problems with balance and cataracts. As this mutation is novel, literature is extremely limited, especially on the compound heterozygosity of the mutation, the phenotype described by the University of Oxford and the A927E mutation. Uniprot was used to align the protein sequence of nesprin-3 in a variety of different organisms to assess the conservation of the amino acids implicated in the constructs.

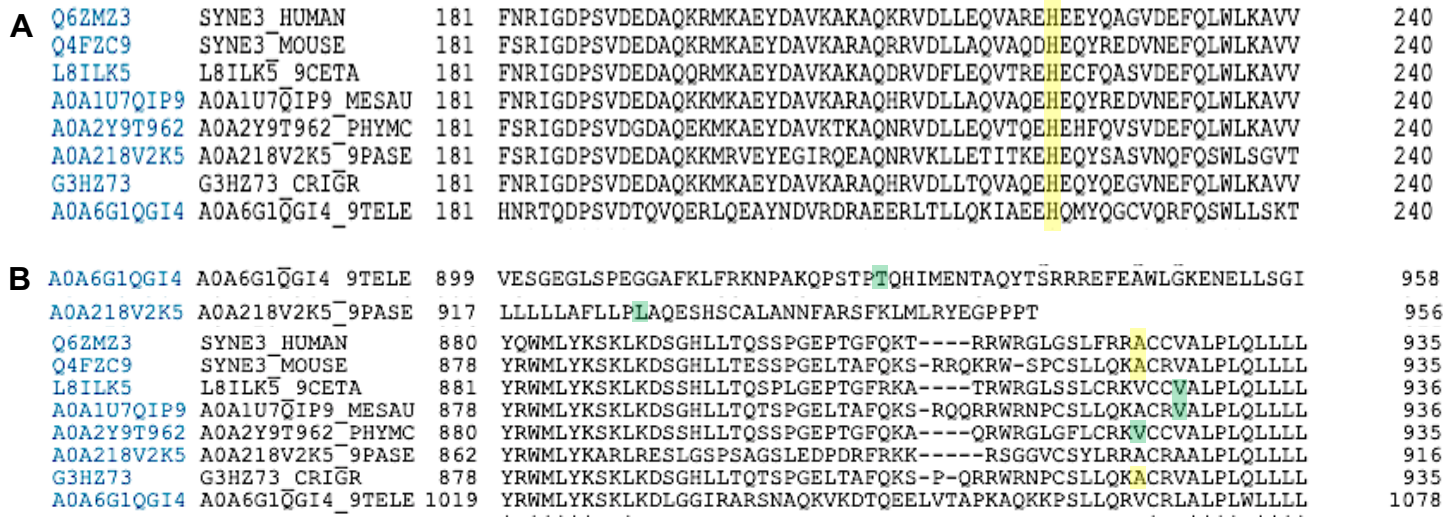

Figure 19 Protein sequence analysis of nesprin-3 showing location 222 (A) and 927 (B). The eight species compared were: human, mouse, wild yak, golden hamster, sperm whale, Bengalese finch, Chinese hamster and northern snakehead. The amino acid histidine is conserved in all eight species at position 222 (A). The amino acid alanine however is only conserved in three of the eight species. Amino acids highlighted in yellow are histidine and alanine at position 222 and 927. The green highlight shows different amino acids at position 927 where alanine should be.

Figure 19 highlights the different findings of the protein sequence analysis search completed for the nesprin-3 mutation constructs. The protein sequence for eight different species was aligned using BLAST and the amino acids at position 222 and 927 compared. Figure 19A shows the amino acid histidine at position 222 highlighted in yellow. This amino acid was conserved at the same position in all eight species. When compared to alanine at position 927, it was found that the amino acid was only present at that specific location in three of the eight species, highlighted in yellow in Figure 19B. Five of the eight species had amino acids other than alanine at position 927, highlighted in green. In summary, it suggested that histidine at position 222 within spectrin repeat 2 is conserved when compared to alanine at position 927 within spectrin repeat 8.

3.10.1 Nesprin-3 H222Y overexpression does not promote MACF1a3 recruitment to the nuclear envelope

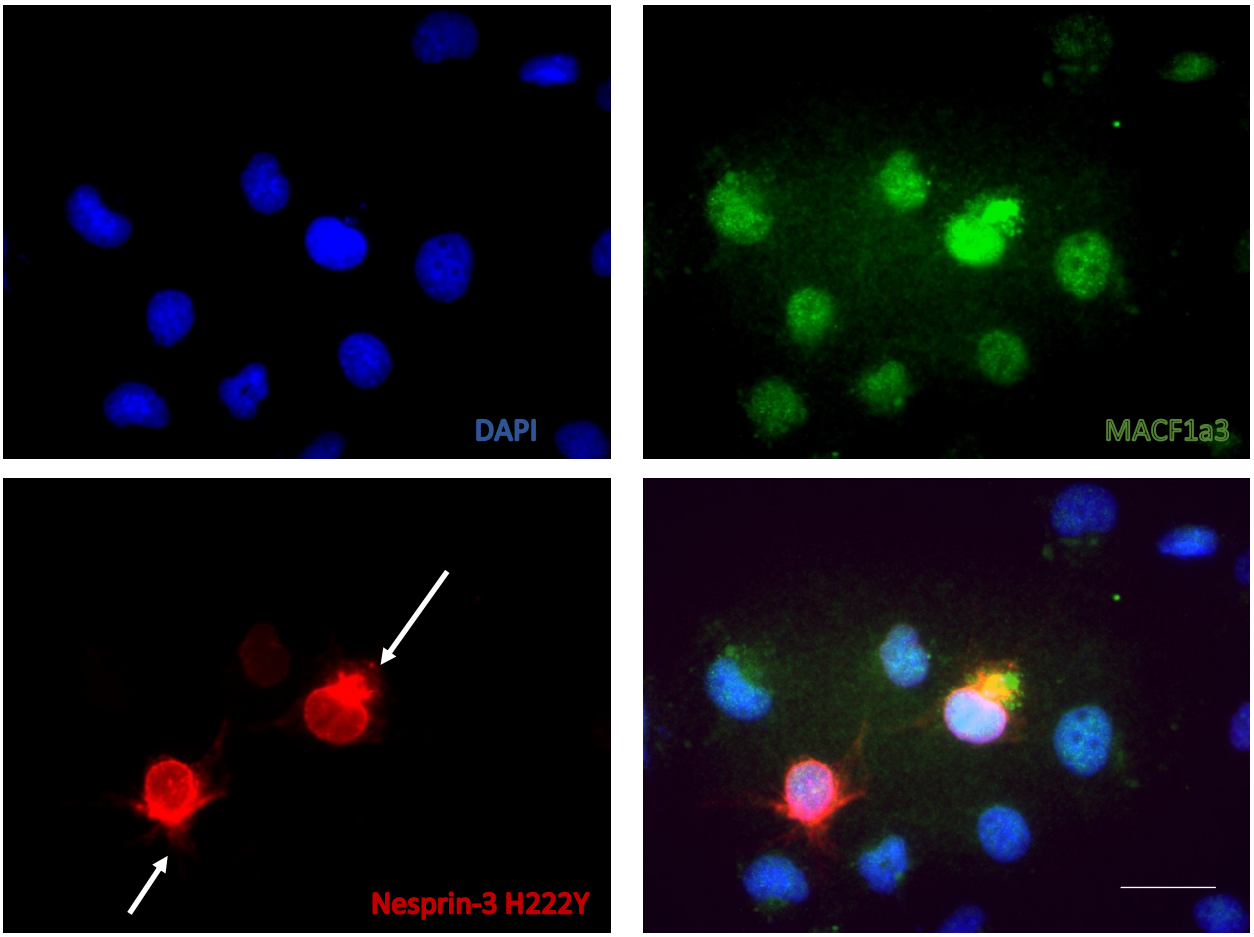

Figure 20 Transfection of COS-7 cells with nesprin-3 H222Y to assess its ability to recruit MACF1a3 to the nuclear envelope. COS-7 cells were transfected with myc-tagged mutant nesprin-3 'H222Y' plasmid. Cells grown and fixed and imaged on Zeiss Axiovision microscope. Transfected COS-7 cells overexpressing H222Y nesprin-3 could not recruit MACF1a3 to the nuclear envelope. Scale bars: 25μm

COS-7 cells were transfected with the H222Y nesprin-3 plasmid and grown to a 70% confluency before being fixed. The data and images produced demonstrated that similarly to WT nesprin-3 in Figure 20, H222Y nesprin-3 was also unable to recruit MACF1a3 to the nuclear envelope. For MACF1a3, the staining seen in the figure above does not show any nuclear envelope rings or patterns. Instead, the staining appears to be cytoplasmic. This particular coverslip shows two COS-7 cells that have been successfully transfected. Two main observations

can be made from this image. The first is that the transfection appears to have worked in the two cells, albeit only partially as the other cells in the same image have not been transfected. The second is that although it is clear to see there is a ring around the nuclear envelope where it would be expected, there are also some changes which can be seen in the transfected cells. The arrows in Figure 20 point to structures on the cell which look like nuclear protrusions and may possibly be the microtubule organising center (MTOC). Furthermore, another finding which was observed whilst examining the transfected cells was that some of the nuclei appeared to have a more disturbed shape when compared to the WT. Although this was not quantified and examined further due to the time constraints of the project, it would be an interesting area to research further. One explanation for this however may be that the cells simply did not survive the transfection process and were in the process of degradation. In summary, neither the WT nor H222Y nesprin-3 were able to recruit MACF1a3 to the nuclear envelope. Following this, plectin recruitment to the nuclear envelope was assessed through transfection of COS-7 cells with WT nesprin-3α and H222Y, and also with A927E.

3.10.2 Overexpression of WT and H222Y Nesprin-3 promotes plectin recruitment to the nuclear envelope.

As previously demonstrated in many previous papers and studies, it is known that nesprin-3α can interact with plectin and that their interaction is specific. As nesprin-3α lacks an ABD, it is not able to interact and associate with actin but can interact with the cytoskeleton through plectin (Wilhelmsen et al., 2005). In this project, the recruitment of plectin by a WT nesprin-3 and mutant nesprin-3 constructs H222Y and A927E was studied. To assess the possible difference in recruitment of plectin by H222Y and A927E nesprin-3, it was necessary to assess how the WT form of the protein behaved. The results are shown in Figure 21 below.

A

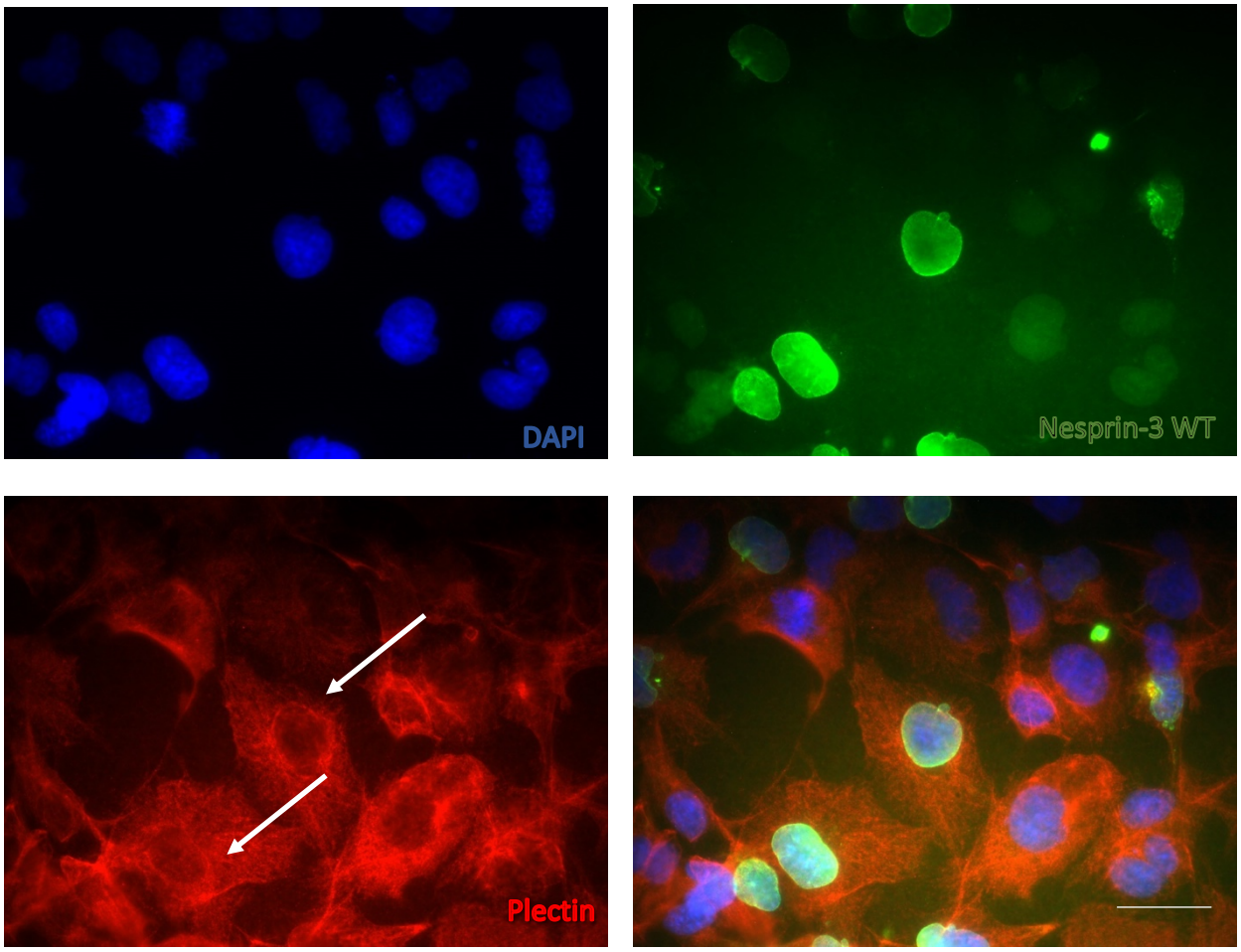

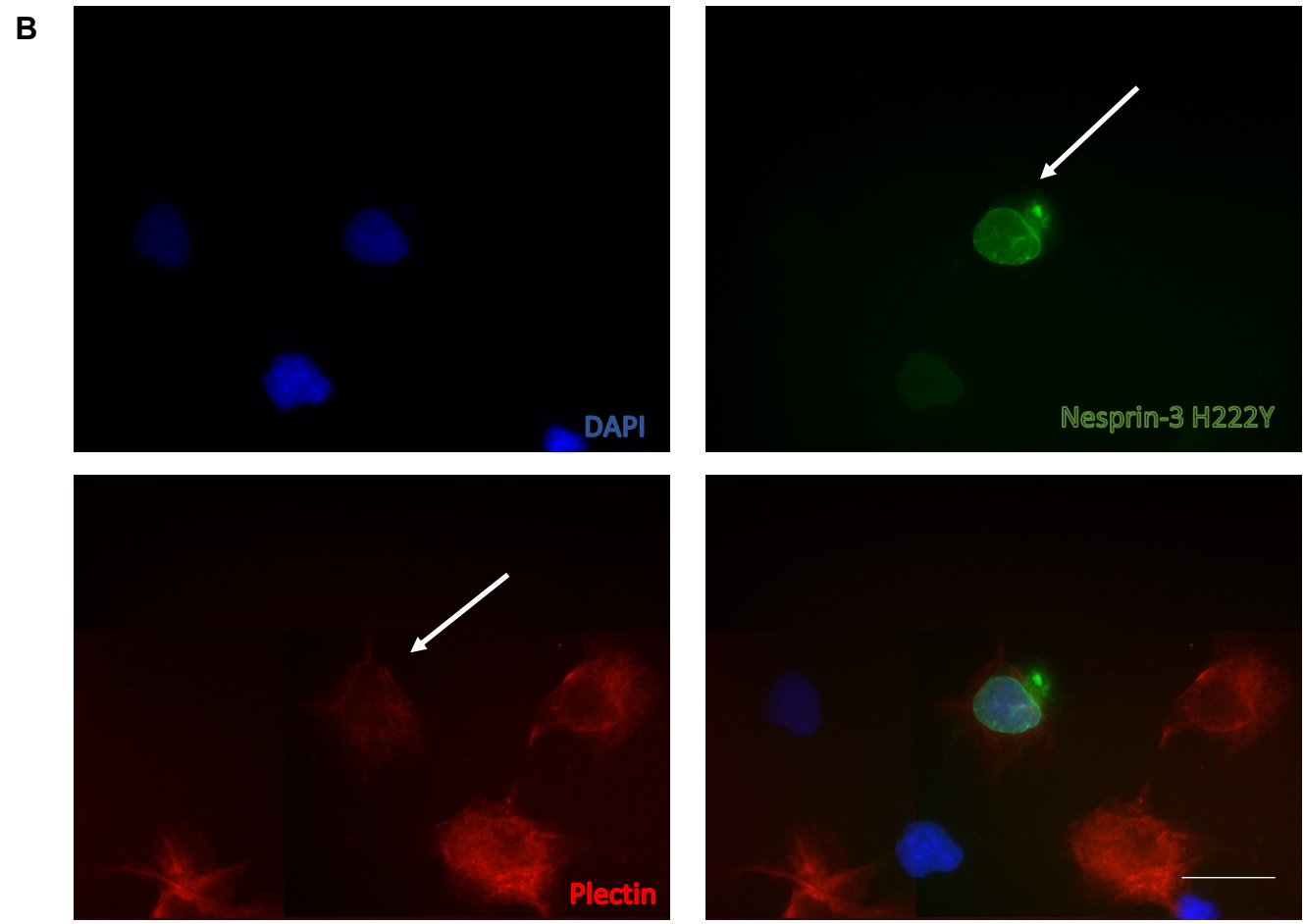
B
DAPI
Nesprin-3 H222Y
Plectin

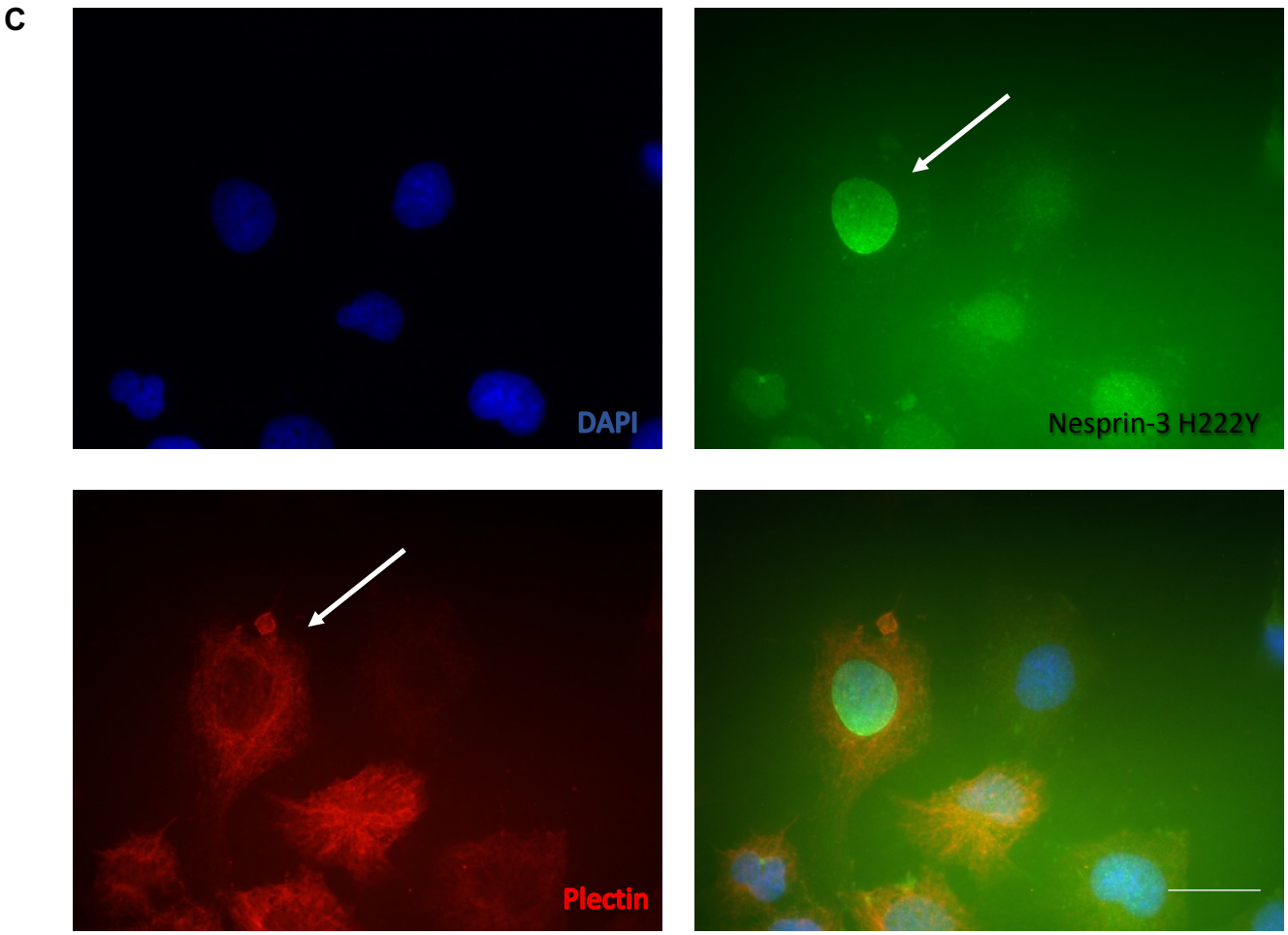
C
DAPI
Nesprin-3 H222Y
Plectin

Figure 21 Images showing transfection of COS-7 cells with WT nesprin-3 and H222Y nesprin-3 to assess ability to recruit plectin. A) Transfected WT nesprin-3 able to recruit plectin to the nuclear envelope. B) Transfected H222Y nesprin-3 unable to recruit plectin to the nuclear envelope. C) Example of H222Y nesprin-3 positively recruiting plectin to nuclear envelope. Scale bars: 25μm

This transfection used a myc-tagged WT nesprin-3 plasmid. The images in Figure 21A show that although a full transfection was not achieved, there was a sufficient number of transfected cells to be able to quantify the results. A total of 300 transfected and 300 untransfected cells were counted and the results plotted to produce the graph in Figure 22B based on whether they had or had not recruited plectin to the nuclear envelope. Examples of plectin recruitment by the transfected cells are highlighted using arrows. The data collected in Figure 22B showed that the WT nesprin-3α was largely unable to recruit plectin to the nuclear envelope. As was demonstrated previously in Figure 16C, COS-7 cells did not express the full length nesprin-3. Therefore, this can explain why an untransfected cell which is not overexpressing nesprin-3 cannot recruit plectin. This finding is also supported by a study carried out by Taranum et al., (2012) in which they have a similar discovery that an overexpression of nesprin-3 in COS-7 cells achieves recruitment of vimentin filaments to the nucleus.

Similarly, our data showed that following an overexpression of nesprin-3α, approximately 70% of the transfected cells were able to recruit plectin to the nuclear envelope. Furthermore, in the transfection with WT nesprin-3α, we found that plectin shape and size was unchanged. This is contrary to what we found in the transfection with H222Y nesprin-3 which will also be discussed. In summary, the data produced here demonstrated a baseline for the later experiments and showed that an overexpression of nesprin-3α can stimulate and increase the rate of recruitment of the plectin protein to the nuclear envelope.

The same model of experiment was repeated for H222Y nesprin-3. Figures 21B, 21C and 22B show a summary of the data gathered. The data demonstrated that although H222Y nesprin-3 was still able to recruit plectin to the nuclear envelope, its ability to do so was reduced

compared to the WT nesprin-3. The level of recruitment in WT nesprin-3α was approximately 70% compared to approximately 37% in the H222Y nesprin-3. Once more, 300 cells which were transfected were quantified based on whether they had or had not recruited plectin. An example of a cell which was transfected and had recruited plectin to the nuclear envelope is shown with arrows in Figure 21C and a cell which was transfected but was not able to recruit plectin shown in Figure 21C. 300 untransfected cells were also counted. The results were plotted, and the graph shown in Figure 22B was produced. An interesting observation that arose from this experiment was that although a mutant form of nesprin-3 was tested, it showed that it was still able to an extent to carry out one of its functions which is the recruitment of plectin.

A second observation which was made was that although plectin was recruited, Figure 21C shows that the staining around the nuclear envelope is not as strong as in the WT nesprin-3α in Figure 21A. This may be due to the mutated nesprin-3 having a dampened ability to bind to plectin properly and hence the strength of the binding may be reduced. Moreover, plectin size and shape appeared to be altered by the mutant nesprin-3 shown in Figure 21B compared to WT in Figure 21A. Plectin appears to have be smaller in size and more constricted with a more disturbed structure. Further research on this observation would be valuable as it would allow improved understanding of how a mutant form of nesprin-3 can affect plectin and other cytoskeletal proteins.

3.10.3 Overexpression of nesprin-3 A927E promotes plectin recruitment to the nuclear envelope

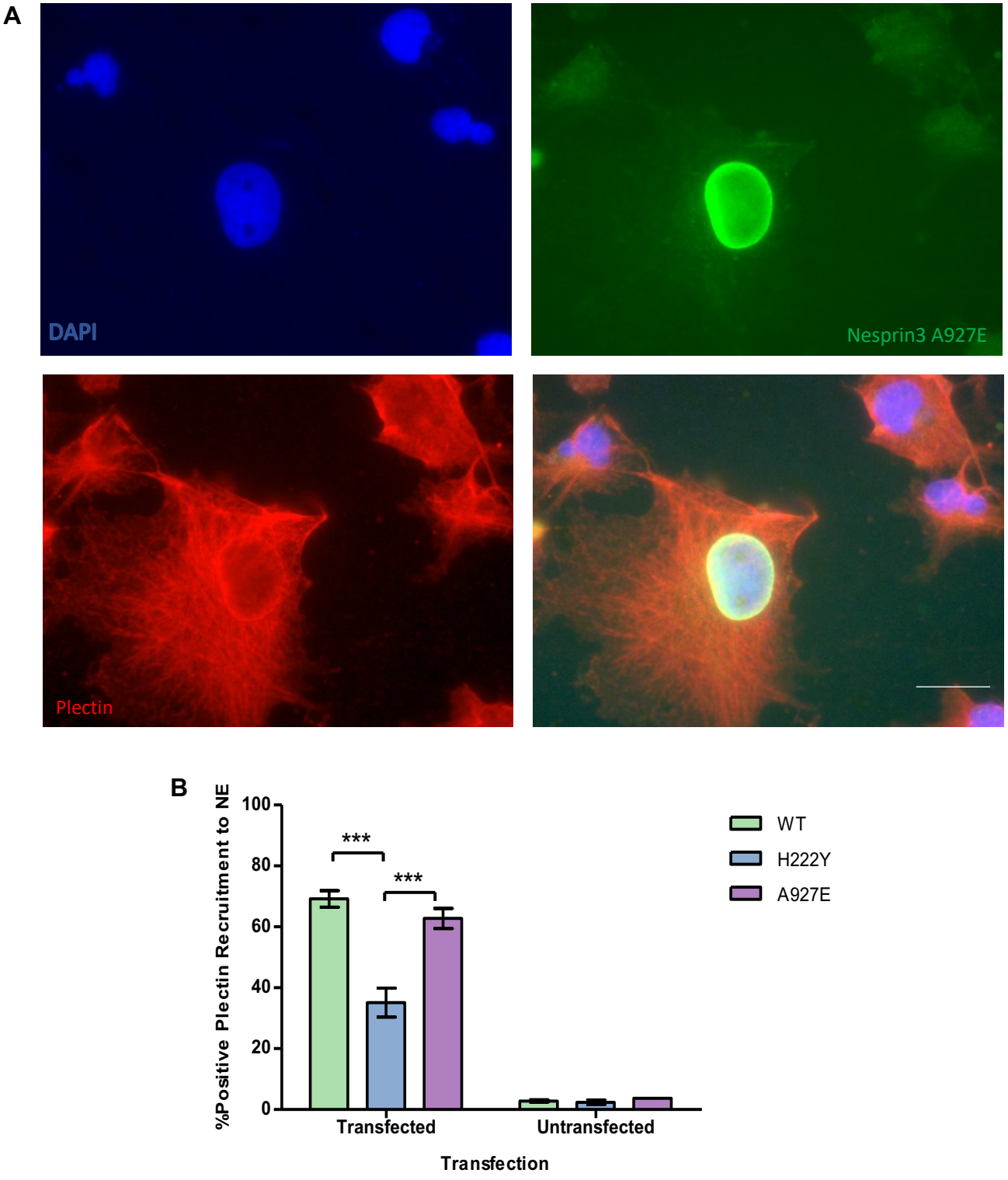

Figure 22 Transfection of COS-7 cells to overexpress Nesprin-3 A927E and assess plectin recruitment. A) Image showing transfected COS-7 cell and nesprin-3 staining around the nuclear envelope. Plectin has been recruited to the nuclear envelope by this transfected cell. B) Graphical summary of plectin recruitment by the three different constructs provided: nesprin-3 WT, H222Y and A927E. Statistical analysis carried out using one-way ANOVA test. *** $P \leq 0.001$. Scale bars: 25μm

The same experiment was repeated with the nesprin-3 A927E constructs provided by the University of Oxford. COS-7 cells were transfected with the constructs to overexpress nesprin-3 A927E and assess its ability to recruit plectin. The image shown in Figure 21A is an example of the type of transfected cell and its recruitment of plectin to the nuclear envelope. To produce the graph in Figure 21B, 300 cells of the type shown in Figure 21A were counted and results plotted based on whether the cells had or had not recruited plectin. The results of the quantification are shown in Figure 21B. The data gathered in this experiment showed that nesprin-3 A927E did have the ability to recruit plectin to the nuclear envelope. When compared with nesprin-3 A927E, nesprin-3 H222Y was less efficient at recruiting plectin to the nuclear envelope. The graphs show that approximately 37% of transfected H222Y cells were able to recruit plectin compared to approximately 50% of transfected A927E cells. Moreover, plectin appeared to have a more normal structure and shape following transfection of A927E when compared to transfection of H222Y. This is shown in Figure 21B in which it is clear to see that plectin shape appears closer to the shape seen in the transfection of nesprin-3 WT in Figure 20A than in the transfection of nesprin-3 H222Y presented in Figure 20C and D.

In summary, the data collected in this set of experiments indicated that all three constructs had the ability to recruit plectin, as shown in Figure 21B. Overexpressing WT nesprin-3α and A927E nesprin-3 resulted in a recruitment level of approximately 70% and 62% respectively. However, H222Y nesprin-3 only achieved a recruitment of plectin in approximately 37% of its transfected cells. Therefore, the ability of this mutated construct to recruit plectin to the nuclear envelope appears to be greatly reduced when compared to WT nesprin-3 and A927E nesprin-3.

4. Discussion

This project began with the initial aim of assessing the expression levels of MACF1a3 in COS-7, HaCaT, C6 and HDF cells and to identify within those cells how MACF1a3 distributes itself in relation to F-actin and microtubules. This was followed by assessing the expression level of nesprin-3 in COS-7, HaCaT, C6 and HDF cells and identifying its distribution pattern within those cell lines. These two steps were carried out to provide an initial understanding of how the two proteins, MACF1a3 and nesprin-3 interact individually within cells. Once expression levels and distribution patterns within cells were established, the next set of experiments into recruitment of MACF1a3 to the nuclear envelope by nesprin-3 was initiated. COS-7 cells were transfected to overexpress nesprin-3 in a WT and mutant form to assess whether recruitment of MACF1a3 to the nuclear envelope by nesprin-3 was possible. Finally, the third cytolinker protein, plectin, was integrated into the experiments. The recruitment of plectin to the nuclear envelope was assessed following transfection of COS-7 cells to overexpress WT nesprin-3 and two mutant nesprin-3 constructs: H222Y and A927E.

4.1 MACF1a3 shows varied expression in COS-7, HaCaT, C6 and HDF cell lines

A gradient gel was used for the MACF1a3 western blot shown in Figure 9 as a lower polyacrylamide concentration was needed to separate the higher molecular weight proteins, in this case MACF1a3 due to its molecular weight of approximately 600 kDa. It was expected that the result would be the detection of one clear band at 600 kDa for each of the cell lines: COS-7, HaCaT, C6 and HDF. Contrary to this, multiple bands were detected at varying molecular weights for each of the cell lines aforementioned. Similar size bands were detected at around 100 kDa in COS-7, HaCaT and HDF cells but not in C6 cells. Contrastingly, similar size bands were detected at 200 and 250 kDa in COS-7, HaCaT

and C6 cells but not in HDF cells. Although there were signals detected using the MACF1a3 antibody in each cell line, interestingly, a strong band was only detected at the 600 kDa mark in COS-7 and HDF cells and very weakly in HaCaT cells. This may suggest that only COS-7 and HDF cells express full-length MACF1a3 when compared with HaCaT and C6 cells. Generally, similar size bands were detected on the blot shown in Figure 9 irrespective of the lysate analysed, the only difference being the detection of bands at each molecular weight in the lysates.

Research on MACF1a3 is limited as it is so specific and much of the literature refers to the protein as simply MACF1, often not distinguishing between the isoforms. Hence, it was difficult to find similar research conducted into the MACF1a3 protein in the same cell lines, COS-7, HaCaT, C6 and HDF cells, which we used, in order to find comparative results. However, the findings of Figure 9 can be supported by previous literature and research into the MACF1 protein, albeit not the specific MACF1a3 isoform this project focussed on. The strongest expression of MACF1a3 at the molecular weight of 600 kDa was found in HDF cells. Therefore, this indicates that there is an abundance of the MACF1a3 protein in fibroblast cells. A study by May-Simera et al., in 2016 in which they caused a deletion of MACF1 in immortalised mouse embryonic fibroblasts highlights both the presence and function of MACF1 in fibroblasts. Following the deletion of MACF1 and upon serum starvation, ciliogenesis was abolished. The implications of ciliogenesis abolishment are that cilia cannot be produced. Ciliary defects lead to a variety of human diseases such as hydrocephalus and kidney disease (Badano, Mitsuma, Beales and Katsanis, 2006). This is one example which highlights not only the presence of MACF1 in fibroblasts but also one of its roles within the cells and the implications on general health and disease if its function is not fulfilled.

The second strongest expression of full-length MACF1a3 was detected in COS-7 cells in Figure 9. A similar result was also previously reported in a study by Lin in 2005. In this study, they prepared an antibody which

they named CU119, that was capable of recognising two MACF1 isoforms: MACF1a and MACF1b by recognising the full length plakin domain of MACF1. Although this portion of their work was carried out to test the specificity of their antibody primarily, they demonstrated to a similar strength seen in Figure 9 of this project, that COS-7 cells do express MACF1a. A northern blot analysis by Lin in 2005 using labelled cDNA probes that recognised the plakin domain of MACF1a also showed a strong expression of MACF1a in kidney cells. Thus, this work may validate the band detected at 600 kDa in COS-7 cells, shown in Figure 9.

Furthermore, they also analysed the presence of MACF1 in HaCaT cells. Although this project assessed the presence of MACF1a3 in HaCaT cells, the research mentioned here carried out by Lin in 2005 focussed on MACF1b. They found that following the creation of a lysate from HaCaT cells and subjecting it to immunoblotting with their CU149 antibody, specific to MACF1b, a faint band was detected. This band appears similar in size and strength to the band detected in HaCaT cells in Figure 9. From this, it is possible to suggest that the expression of MACF1 does not differ drastically in strength between isoforms MACF1a3 and MACF1b. Interestingly, (Lin, 2005) describes a relationship between MACF1 and the Golgi complex which may offer one explanation as to the faint band detected in HaCaT cells when compared to the stronger bands detected in COS-7 and HDF cells. They isolated Golgi and endoplasmic reticulum fractions in human lung carcinoma (H460) cells and found that MACF1b was primarily detected in the Golgi fraction when compared with detection in the endoplasmic reticulum fraction. In immunofluorescence experiments, they also found that MACF1b colocalises with the Golgi complex in HaCaT cells. HaCaT cells are human epidermal keratinocyte lines and keratinocyte differentiation has been shown to promote and result in the dispersal and fragmentation of Golgi (Mahanty et al., 2019). Therefore, one possible explanation for the weaker expression of MACF1a3 in Figure 9 and MACF1b in the study by Lin in 2015 in HaCaT cells may be that

increased differentiation of HaCaT cells which leads to a loss of Golgi proteins could also lead to a reduction in MACF1a3 levels as they are colocalised to Golgi proteins. This would be an interesting area to further research as there is no evidence in current literature of a MACF1a3 relationship with the Golgi complex, similar to MACF1b, which may possibly provide a more robust explanation for the reduced expression of MACF1a3 in HaCaT cells.

Unexpectedly, there was no expression of MACF1a3 in C6 cells at a molecular weight of 600 kDa in Figure 9. C6 glioma cells are produced by cloning rat glial tumours. Glial cells are non-neuronal cells in the brain and spinal cord. When injected into the brain of neonatal rats, C6 cells can stimulate human glioblastoma multiforme (GBM), which is the most aggressive glioma tumour. Similar cell lines include U251 and A172, which will also be discussed (Giakoumettis, Kritis and Foroglou, 2018).

Early research into the MACF1 proteins by Bernier et al. in 1996 demonstrated expression levels of MACF1 in various tissues. Through the use of RNase protection assays, a method which measures the abundance of specific mRNAs in samples of total cellular RNA, they tested a number of mouse tissues including brain, lung, kidney and skin. This technique, carried out on mice three days old, showed that the MACF1 expression was strongest in the lung, followed by the brain and spinal cord. Although they used northern blotting techniques in this experiment, and we have used western blotting, the goal of both experiments was to identify the expression level of MACF1. Strong expression of MACF1 was detected in mouse brain and spinal cord tissues in the study by (Bernier et al., 1996), and as C6 glioma cells were used in this project, it was expected that a similar expression would be seen in the western blot analysis. In addition to this, recent literature has also identified MACF1 as a potential novel target in glioblastoma. Research conducted by Afghani et al. in 2016 identified MACF1 expression presence and increase in astrocytoma tissue taken from tumour patients and also glioblastoma cell lines such as A172

when compared to normal controls by western blotting. Furthermore, Afghani et al also demonstrated that MACF1 downregulation with RNA interference resulted in a reduction in the proliferation and migration of glioblastoma cells, hence implicating MACF1 as positively influencing the ability of glioblastoma cells to proliferate and migrate.
Due to these studies and findings, it would be difficult to suggest that C6 cells do not also express MACF1a3 at the full length of 600 kDa. The lack of bands at this molecular weight may then be due to a number of factors, from cell culture and protein lysate quality, to western blotting technique, transfer time and detection. Further improvement on these techniques and experiment repeats may yield improved and expected results as to expression of MACF1a3 in C6 cells.

Furthermore, Figure 9 shows that a range of bands were detected in COS-7, HaCaT, C6 and HDF cells at varying molecular weights for the MACF1a3 protein. It is usually reported that multiple bands detected on a western blot may be due to protease degradation or too many passages of cell lines resulting in differences in their protein expression profiles. However, in this instance, the most feasible explanation is that the multiple bands detected are due to different splice variants being detected by the anti-MACF1a3 antibody. A group who commented on the same finding in their results is Bernier et al. in 1996, attributing the multiple signals in one lane not to protein degradation but to the presence of aberrant splice products. This specific experiment shown in Figure 9 was repeated many times and originally produced no signals. The antibody dilutions were increased gradually until some signal was produced and then finalised. Initially, the same multiple band pattern was found in in COS-7, HaCaT, C6 and HDF cells. Due to this, it was suggested that the anti-MACF1a3 antibody used was not specific. Thus, the silencing experiment shown in Figure 14 was carried out, of which one of its aims was to test the specificity of the antibody. A partial knockdown effect was observed in siRNA #2, detected by the anti-MACF1a3 antibody, hence suggesting that the antibody was in fact specific. Moreover, as the multiple bands were detected in all four cell

lines, COS-7, HaCaT, C6 and HDF, in old and fresh lysates tested (not shown) and the blot was repeated many times, it is unlikely that the cause is due to cell culture or lysate production but rather there were splice products being detected by the anti-MACF1a3 antibody. A suggestion for improvements on similar future experiments may be to test the different types of polyacrylamide gels available and the running time of the gel to more accurately pick out the higher molecular weight bands belonging to MACF1a3 and limit detection of possible non-specific bands or splice products.

4.2 Immunofluorescence staining and Western blot analysis of MACF1a3 expression in COS-7, HaCaT, C6 and HDF cells showed similar patterns

Previous literature has shown that MACF1 can associate with actin in its polymerised form as F-actin. This was demonstrated by Karakesisoglou, Yang and Fuchs in 2000 in which they combined polymerised actin with a GST-MACF1 fusion protein, producing a binding of F-actin with the actin binding domain of MACF1. Moreover, as the concentration of MACF1 increased, they reported an increased saturation of MACF1's association with polymerised actin. This was further confirmed in vivo by transfection to express an HA-epitope-tagged actin binding domain of MACF1 in SW13 cells that lack a cytoplasmic IF network. The results of this transfection showed that HA-specific antibodies and anti-β-actin colocalised with stress fibres and the cortical cytoskeleton. MACF1 also associates with microtubules. Karakesisoglou, Yang and Fuchs, 2000 showed that in epidermal cells, MACF1 binds along microtubules and concentrations at the (+)-ends of microtubules which are directed towards migrating cell edges. The relationship between MACF1 and microtubules was further established through experiments with MACF1 knockout cells. MACF1 knockout induced a change in microtubules including irregular trajectories, curling and bending at cell margins. Knockout microtubules that

reached the plasma membrane failed to tether themselves to the membrane, instead continuing to grow, bend and curl. Interestingly, it was reported that MACF1 knockout in this study had little effect on the actin cytoskeleton. In vivo, microtubules are stabilised and guided by the actin cytoskeleton from the microtubule organising centre (MTOC) to the cell periphery. As the links between MACF1, actin and microtubules are well established, one aim of this project was to assess whether any patterns could be observed between MACF1, actin and microtubules in COS-7, HaCaT, C6 and HDF cells.

4.2.1 COS-7, HaCaT, C6 and HDF cells exhibited different staining patterns for MACF1a3

The major observation made from the staining of MACF1a3 in COS-7, HaCaT, C6 and HDF cells was that they varied distinctly from each other, possibly reflecting the strength of expression of MACF1a3 in Figure 9.

HDF cells showed filamentous, track like staining for MACF1a3 whereas in COS-7 cells, MACF1a3 appeared to be ‘dotty’ and cytoplasmic. MACF1a3 staining in HaCaTs was observed strongly in the nucleus. Although C6 staining was faint, it was possible to see that MACF1a3 was present in the form of ‘dotty’ cytoplasmic structures and through the nucleus. As the staining pattern between each cell line is so varied, it is difficult to come to a conclusion about one pattern of MACF1a3 staining which is the same in COS-7, HaCaT, C6 and HDF cells. One explanation for this may be that MACF1a3 may have differing roles and functions within each of the four cell lines, making it necessary to have different localisation patterns. For example, it may be colocalising with a variety of different structures within cells. One of these may be mitochondria. It was suggested that MACF1a3 may be colocalising with mitochondria in HDF cells, and thus a short experiment into this hypothesis was conducted, the results of which are shown in Figure 15. The arrows in this figure point to possible sites of co-

localisation. However, due to time constraints on this project, it was not possible to carry out co-localisation studies to assess for definite whether MACF1a3 was co-localising to mitochondria. Furthermore, as discussed previously, it has been demonstrated that another MACF1 isoform, MACF1b colocalises with Golgi. Therefore, it may not be incorrect to suggest that MACF1a3 may be doing the same either with Golgi or another intracellular component. To further research this, it may be useful to carry out cell fractionation studies and further immunofluorescence studies. Regarding F-actin, Figure 10 showed that there was no evidence of co-localisation between MACF1a3 and F-actin, stained by TRITC-phalloidin. The antibodies here produced different staining patterns for the proteins and as such, a strong overlap between the two could not be found. This finding may be explained by the domain structure of MACF1a3. As the protein lacks CH1 and only has CH2, its binding affinity to actin filaments is reduced. Thus, it may be more difficult to establish an association between MACF1a3 and F-actin that would be strong enough to be detected under a microscope. However, in Figure 13A and B, the arrows point to areas of the merged images of MACF1a3 and microtubules, in HDF and COS-7 cells respectively, that may possibly contain regions of co-localisation. Once again, this statement would benefit from further repeats and imaging using confocal microscopy and co-localisation techniques. It is also possible however that no co-localisation was taking place and the colour change to yellow may simply have been due to the overlap of the fluorophores.

Achieving high quality staining in COS-7, HaCaT, C6 and HDF cells was a difficult and lengthy process as the antibodies used in the first instance were not producing signals. The protocol had to be adapted and repeated many times to achieve the images shown in Figures 10 and 12. However, there was still discrepancy between the cell lines in regard to how well the anti-MACF1a3 antibody worked. In COS-7 and HDF cells, structures were easy to detect and image and did not have a lot of background stain. In contrast, HaCaT cells were the most

difficult to stain for MACF1a3, detect and image as there was consistently high background regardless of the antibody concentrations used or number of washes. It was also difficult to identify cytoplasmic structures as the stain appeared to be concentrated in the nucleus. The western blot in Figure 9 may offer an explanation for this. The strongest expressors of MACF1a3 at 600 kDa were COS-7 and HDF cells, the same cells which produced the best quality immunofluorescence stain by the same anti-MACF1a3 antibody. On the other hand, there was very weak expression of MACF1a3 in HaCaT and C6 cells on the western blot, reflecting the weak signals achieved by the anti-MACF1a3 antibody in immunofluorescence images. Future studies may benefit from experimenting further with antibody dilutions and washing steps following fixation to achieve an improved staining quality and sharper images.

4.3 Assessing nesprin-3 expression in COS-7, HaCaT, C6 and HDF cells with Western blotting

Nesprin-3 was first discovered by Wilhelmsen et al. in 2005 when attempting to find other proteins which could bind to the plectin ABD. Through a yeast two-hybrid screen with the ABD of plectin-1C as bait, nesprin-3 was isolated. Nesprin-3 was the first ONM protein that had an established link to the IF cytoskeletal system through its association with plectin. The domain structure of the two known isoforms of nesprin-3 in mice is shown in Figure 16A. At the time, research into this novel protein was limited and the group suggested that the discovery would increase knowledge of the function of nesprin-3 and the NE in relation to mitosis and nuclear positioning during cell migration. Literature surrounding nesprin-3 has since become abundant and this project aimed to fill in some gaps still present. Investigating whether overexpression of nesprin-3 would promote the recruitment of MACF1a3 to the nuclear envelope was one of these aims.

4.3.1 HDF cells expressed full-length nesprin-3α

The first step in this series of experiments was to assess the expression levels of nesprin-3 in COS-7, HaCaT, C6 and HDF cells to provide a foundation of knowledge surrounding the cells used and which would be most appropriate to carry through to future studies. As nesprin-3 is ubiquitously expressed in all cells and tissues (Wilhelmsen et al., 2005), it was expected that expression bands would be detected in COS-7, HaCaT, C6 and HDF cells by Western blotting. Interestingly, following repeats of protocol and changing of antibody dilutions, expression of full-length nesprin-3 was only detected in HDF cells. Previous literature may be used to provide an explanation for the lack of expression of nesprin-3 in some of the cells we tested. In 2012, Taranum et al stated that COS-7 cells were almost devoid of nesprin-3 in vitro. This statement is backed up by a Western blot analysis of untransfected COS-7 cells tested for expression of nesprin-3 versus nesprin-3α cDNA-transfected and nesprin-3β cDNA-transfected COS-7 cells by Wilhelmsen et al in 2005. The results showed that untransfected COS-7 cells produced almost no signal through western blotting for nesprin-3 versus a strong signal for nesprin-3α cDNA-transfected and cDNA-transfected COS-7 cells. Thus, the lack of expression of nesprin-3 in the COS-7 cells used in this project fits what has been observed in previous research and literature.

Figure 16C also showed a lack of nesprin-3 expression in HaCaT cells. Although the results which show this lack of expression in this project come from western blotting and immunofluorescence techniques, other groups have also commented on the lack of nesprin-3 expression in certain cells, including keratinocytes and hepatocytes via different methods. Ketema et al. in 2013 stained tissue sections of wild-type and nesprin-3 knockout mice for nesprin-3 and plectin. Their results demonstrated a normal expression of plectin in keratinocytes and hepatocytes compared to a lack of expression of nesprin-3. This finding may be used to support the lack of expression of nesprin-3 in the HaCaT cells used in this project. Moreover, they state that nuclear

envelope staining and presence of nesprin-3 was weak in cardiac muscle, only occasionally detected in skeletal muscle and expression decreased during myogenic differentiation.

A lack of expression of nesprin-3 was also found in C6 cells. This contradicts the data presented in the form of an image of a C6 cell stained with an anti-nesprin-3 antibody in Figure 17A. The image shows clear expression of nesprin-3 around the nuclear envelope in the form of a nuclear envelope ring. As the same antibody and C6 cells were used both in the immunofluorescence and western blotting experiments, it was expected that nesprin-3 would also be detected in C6 cells through western blotting. As the concentration of the anti-nesprin-3 antibody was increased gradually to produce a signal for the immunofluorescence experiments and produce the image shown in Figure 17A, a suggestion would be to increase the antibody concentration for future western blotting experiments as the dilution may have been too weak during the incubation stage to later detect a signal in C6 cells for nesprin-3.

Interestingly, there were bands detected in COS-7, HaCaT, C6 and HDF cells below 72 kDa, presented in Figure 16C. Originally, it was suggested that the anti-nesprin-3 antibody could be detecting bands belonging to nesprin-3β. However, this does not fit the molecular weight the bands were detected at as nesprin-3β has a molecular weight of approximately 102 kDa. This finding was not unique to this project, however. A number of groups have found that their anti-nesprin-3 antibody also detects bands at lower molecular weights in certain cells (Ketema et al., 2013, Postel et al., 2011 and Wilhelmsen et al., 2005). Wilhelmsen et al suggested that the 97 kDa protein reacting with their nesprin-3 antibody may have been a degradation product of the nesprin-3 protein. This is one possible explanation as to why multiple bands were also detected in Figure 16C. Another possible explanation may be that there is presence of an isoform which is yet to be

discovered, being detected by the anti-nesprin-3 antibody. As discussed in the results section, the genomic database Uniprot identifies three different isoforms of human nesprin-3 produced by alternative splicing, the smallest being the third isoform at 69 kDa. Hence, it may be possible that there are more isoforms present in mice for nesprin-3 than are currently identified and reported on.

4.3.2 Immunofluorescence studies showed varying levels of nesprin-3 expression in COS-7, HaCaT, C6 and HDF cells

Testing COS-7, HaCaT, C6 and HDF cells for the presence and localisation of nesprin-3 yielded varying results. In C6 cells, nesprin-3 was found around the nuclear envelope. HDF cells were stained around the nuclear envelope but there was also cytoplasmic stain throughout the length of the cells. HaCaT and COS-7 cells did not show any nuclear envelope staining, instead there was staining all throughout the cells. Due to this variance, it is difficult to state that there was a clear pattern observed amongst all four cell lines with regards to the staining of nesprin-3. HDF cells produced the strongest staining for nesprin-3 in the immunofluorescence experiment, reflected also by its strong expression for nesprin-3 in Figure 15C. HaCaT and COS-7 cells did not express full-length nesprin-3, also reflecting the weak staining presented in Figure 17.

As discussed above, nesprin-3 was present at the nuclear envelope in C6 cells but there was no expression detected in the western blot analysis. There were some limitations with regards to the production of high-quality staining of nesprin-3 in the four cell lines. Firstly, the process of finding a dilution for the anti-nesprin-3 antibody that would give adequate staining which would be picked up by the microscopes was a lengthy one and often yielded no results. This may provide one explanation for the lack of specific staining of nesprin-3 around the nuclear envelope in the four cell lines. However, the most likely explanation may be that the cells chosen in this project simply do not express high levels of endogenous nesprin-3.

4.3.3 Overexpression of Nesprin-3 in COS-7 cells did not promote recruitment of MACF1a3 to the nuclear envelope

To investigate the relationship between nesprin-3 and MACF1a3 and whether there is an association between them at the nuclear envelope, COS-7 cells were transfected to overexpress WT nesprin-3. As COS-7 cells do not express endogenous nesprin-3, the efficiency of the transfection with a myc-tagged WT nesprin-3 construct was easily observed. Research has previously described an interaction between nesprin-3 and MACF. Wilhelmsen et al in 2005 coexpressed cDNAs of VSV-nesprin-3α (vesicular stomatitis virus) and nesprin-3β with cDNA encoding a HA-tagged MACF ABD to test the ability of nesprin-3 to bind to the MACF ABD. Immunoprecipitations were then prepared with anti-HA antibodies and the results showed that nesprin-3α and nesprin-3β could both interact with the MACF ABD. Moreover, they stated that the interaction between nesprin-3α and the MACF ABD was stronger than the interaction between nesprin-3β and the MACF ABD. This suggested that the first spectrin repeat of nesprin-3α, which is missing from nesprin-3β, is crucial for the high affinity of binding of nesprin-3 to ABDs. Following this, the group overexpressed GFP-nesprin-3α and nesprin-3β in COS-7 cells and stained the transfected cells for endogenous MACF and microtubules. Results from this study showed that although microtubules were at the nuclear perimeter, to which MACF can be associated, nesprin-3α could not recruit MACF to the nuclear perimeter, indicating that nesprin-3α and MACF do not associate in cells.

One of the aims of this project was to examine this hypothesis but with the third isoform of MACF1: MACF1a3. The results of this experiment are presented in Figure 18.

Similarly to the study by Wilhelmsen et al in 2005, upon transfection of COS-7 cells with myc-tagged, WT nesprin-3α, no recruitment of MACF1a3 could be detected. One explanation for this lack of

recruitment may be that MACF1a3 is competing with other cytolinkers such as plectin for an interaction with nesprin-3. In the same study by Wilhelmsen et al in 2005, they tested this hypothesis further. Their study used keratinocytes with epidermolysis bullosa simplex with muscular dystrophy (EBS-MD), cells which do not express full-length plectin but do express rodless variants of plectin at low levels. They overexpressed both GFP-Nesprin-3α and nesprin-3β and hypothesised that if there was any competition between MACF and plectin, it would show in this experiment as plectin would not be able to interact with nesprin-3 as strongly and there may instead be a recruitment of MACF by nesprin-3 at the ONM. The results indicated that although there was only a weak interaction between nesprin-3 and MACF in the yeast two-hybrid study, they did observe an increase of MACF staining around the nuclear perimeter in these keratinocytes compared with the PA-JEB cells they used in their earlier studies. PA-JEB cells are 'pyloric atresia associated with junctional epidermolysis bullosa' keratinocytes which do express full length plectin. To summarise this finding, it is possible that nesprin-3 would be able to have some interaction with MACF if a full knockdown of plectin could be achieved, as the interaction between plectin and nesprin-3 is specific. It is also possible MACF is in competition for binding to nesprin-3 with not only plectin, but also actin. Data from the same study by Wilhelmsen et al in 2005 showed that nesprin-3 and actin filaments both compete for binding to plectin. Using latrunculin B, a drug which disrupts actin organisation by sequestering G-actin and preventing F-actin assembly, they demonstrated that there was an increased amount of plectin available to interact with nesprin-3 at the ONM. The hypothesis that plectin recruitment to the ONM is dependent on the presence of nesprin-3 was also studied via the expression of a nesprin-3 siRNA vector in the cells. The result of this experiment was that there was indeed a reduction in the amount of plectin present at the nuclear perimeter and that they were instead distributed in the cytoplasm.

Competition with plectin may be one reason why MACF1a3 does not have the ability to associate with nesprin-3 and be recruited to the nuclear envelope. The second reason may be due to the structure of MACF1a3 itself, presented in Figure 8B. One of the unique features of MACF1a3 is that it lacks half of its actin binding domain: calponin homology domain 1. As an ABD is typically composed of two CH domains (Bañuelos, Saraste and Carugo, 1998), it is likely that lacking one half may have a negative impact on the protein's ability to associate with actin-binding domains of other proteins, such as nesprin-3. This hypothesis was also described in a paper by Jefferson, Leung and Liem in 2004 in which they state that the tandem CH1-CH2 domain has the strongest binding affinity for actin, followed by the CH1 domains by themselves, with the weakest binding affinity belonging to CH2 domains by themselves. As there is competition for association with nesprin-3 from both plectin and actin filaments, it is thus likely that with only the CH2 domain, MACF1a3 would not be able to overcome the competition for association with nesprin-3. BPAG1a3, another member of the plakin family and an isoform of BPAG1, also lacks the first CH1 domain (Jefferson, Leung and Liem, 2006). Whilst nesprin-3 can bind to BPAG1 and BPAG2, which possess both CH2 domains, it cannot bind to BPAG1a3 (Jefferson, Leung and Liem, 2006, Ketema and Sonnenberg, 2011). This suggests that the CH1 domain is crucial for binding to nesprin-3. In addition, as BPAG1 and BPAG2 can bind to nesprin-3, and they are similar in structure to MACF1, it would be expected that MACF1 could also bind to nesprin-3. However, in the paper by Wilhelmsen et al. in 2005, they are not specific regarding which isoform of MACF they have researched, referring to the protein only as MACF. This poses another question: are all the isoforms of the MACF family of proteins unable to associate with nesprin-3? Our results showed that MACF1a3 did not have the capacity to be recruited by nesprin-3α but that does not account for the ability of the other isoforms and would be an interesting area for further research.

4.4 Plectin recruitment to the nuclear envelope is reduced following overexpression of mutant nesprin-3 construct H222Y compared to wild-type nesprin-3 and nesprin-3 H222Y

In addition to testing the recruitment of MACF1a3 by WT nesprin-3α, MACF1 recruitment by nesprin-3 H222Y was also tested, results of which are presented in Figure 20. Similarly to WT nesprin-3α, nesprin-3 H222Y could not promote MACF1a3 to the NE either. As a lack of recruitment of MACF1a3 by both nesprin-3 constructs was established, the next step was to investigate whether the wild-type and mutated nesprin3 constructs were able to recruit plectin to the NE.

Recruitment of plectin by WT nesprin-3 to the nuclear envelope is an event well-studied (Ketema et al., 2007, Wilhelmsen et al., 2005). The binding affinity between nesprin-3 and plectin is specific and it has been stated that alternative sequences preceding the ABD in different plectin isoforms does not have any negative impact on the binding of plectin to nesprin-3 (Wilhelmsen et al., 2005). In this project, this association was studied to provide a baseline for future experiments to allow comparisons to be made with mutant forms of nesprin-3 by transfecting COS-7 cells with a myc-tagged WT nesprin-3α construct. The results of this experiment demonstrated that 70% of transfected WT nesprin-3α cells recruited plectin to the NE.

However, literature is limited surrounding the ability of any mutant forms of nesprin-3 to bind to plectin. In an effort to answer this question, two different mutations of nesprin-3 were given in the form of constructs as part of a collaboration with Oxford University. The mutated constructs, H222Y and A927E were myc-tagged and transfected into COS-7 cells. The results of this study are presented in Figures 21 and 22. As the constructs are mutations of nesprin-3, it would be expected that there would be a deviation from the normal ability of nesprin-3 to recruit plectin. As hypothesised, nesprin-3 H222Y and A927E both had a reduced ability to recruit plectin to the NE compared to the WT nesprin-3 construct.

Surprisingly, there was a large difference in the ability of the mutated constructs to recruit plectin. For example, only 37% of transfected H222Y cells recruited plectin to the NE compared to 62% of transfected A927E cells, data presented in Figure 22B.

The locations of each mutation may offer an explanation for this difference in recruitment ability. Both mutations are missense mutations, single base substitutions at the DNA level, resulting in the coding of a different amino acid at the protein level. The H222Y change is in spectrin repeat 2, exon 4, of nesprin-3α. The exact exon location of the A927E change is not known for definite but it is most likely located between exons 15 to 18 in spectrin repeat 8 of nesprin-3α (Wilhelmsen et al., 2005). Figure 19A shows the histidine amino acid at position 222 conserved between eight different species whereas alanine at position 927 is only conserved in three of the eight same species mentioned in Figure 19B. The highly conserved nature of the histidine amino acid at position 222 indicates that the amino acid must be essential for the maintenance of the structure or function of the nesprin-3 protein or spectrin repeat domain. On the other hand, A927 is less conserved within the eight species, suggesting that the amino acid does not have as essential a function in the protein as H222. Furthermore, research into the spectrin repeats of nesprin-3 and their function further reinforces the finding that the H222Y construct was less able to recruit plectin than the A927E construct due to the location of the mutation.

The plectin-binding domain of nesprin-3α is located within spectrin repeat 1, which is missing from nesprin-3β (Ketema and Sonnenberg, 2011). Two residues, R43 and L44 in the first spectrin repeat of nesprin-3α are essential for the interaction between plectin and nesprin-3, and part of the reason why nesprin-3β cannot interact with plectin (Ketema and Sonnenberg, 2011, Postel et al., 2011). From this, it can be suggested that the location of the H222Y mutation, which is much closer to spectrin repeat 1 than spectrin repeat 8, may have an impact

on spectrin repeat 1, thus reducing the ability of the plectin-binding domain to associate with plectin. Therefore, it can also be stated that the distance between spectrin repeat 1 and spectrin repeat 8 is great enough that a mutation at location 927 has little to no effect on the association of the nesprin-3 protein to plectin.

As this compound heterozygous mutation is unique, there is little in the way of literature to allow for the description and discussion of the mutations and their effects further. The phenotype of this compound heterozygous mutation includes cerebellar ataxia, intellectual disabilities, problems with balance and cataracts (information provided by the collaborators at Oxford University). This phenotype implicates the mutation in major health conditions not previously discussed in literature. As the H222Y and A927E constructs and mutations are novel, literature is limited on any possible health problems they may cause.

A lack of plectin at the nuclear envelope may play a role in the phenotypes described above by the University of Oxford.

Plectin is a versatile cytoskeletal linker protein and it is known to be expressed in a wide range of mammalian tissues and cell types. Plectin can bind to nesprin-3 and simultaneously recruit IFs to the nuclear membrane (Wilhelmsen et al., 2005, Ketema et al., 2007). As stated by Staszewska, Fischer and Wiche in 2015 however, the relevance of these interactions requires further study to establish exactly what their roles are physiologically. Aside from a lack of plectin expression causing EBS-MD (epidermolysis bullosa simplex with muscular dystrophy), Literature has shown that plectin is also involved in chromatin conformation, gene expression, mechanotransduction and anchorage of IF networks. As an example, it has been previously demonstrated that in fibroblasts and keratinocytes, amongst other cells, desmin IF networks form cage-like structures around myonuclei, mechanically connecting and integrating the nucleus with the cytoskeleton. A deficiency of one particular plectin isoform, P1, leads to a decoupling of IFs from the nuclear membrane. Desmin IFs lose their

docking site at the nuclear membrane and collapse onto the surface of nuclei, promoting alterations in nuclear morphology, dislocation of nuclei, decrease in nuclei mobility and impaired mechanotransduction (Staszewska, Fischer and Wiche, 2015). Moreover, their study showed that P1 deficient nuclei migrated over shorter distances when compared with wild-type nuclei. These examples highlight the importance of plectin function within cells and the impact mutations or deficiencies have on wider health.

The phenotype of the H222Y and A927E mutations described the collaborators at the University of Oxford included cerebellar ataxia, cataracts, intellectual disabilities and problems with balance. As these mutations are novel, it is difficult currently to establish exact reasons for these phenotypes. However, literature indicates that LINC complex proteins have been previously implicated in some of these phenotypes mentioned. For example, a mutation in nesprin-1 has been shown to cause a disease referred to as autosomal recessive cerebellar ataxia type I (ARCA-1). This disease is characterised by gait ataxia, oculomotor abnormalities and the presence of cerebellar atrophy following brain imaging (Noreau et al., 2013). Although this refers to nesprin-1, not nesprin-3, it appears to follow a similar pattern phenotypically as what was described by our collaborators. Thus, it is possible that the H222Y and A927E mutations in nesprin-3 may behave in a similar manner as in nesprin-1. However, this hypothesis requires extensive further research. Additionally, the mutations have been shown to result in reduced recruitment ability of plectin to the nuclear envelope. One study by Winter et al. in 2016 has demonstrated that a homozygous mutation in plectin resulting in reduced expression of full-length and rodless plectin showed clinical phenotypes such as bilateral cataracts and brain atrophy. Once more, although in this study, we did not examine plectin mutations, but rather plectin recruitment by nesprin-3 mutated constructs, studies such as the one by Winter et al., 2016 give a good insight into the consequences of a lack of plectin expression. As these mutations are novel, literature is limited and exact

conclusions and reasonings are difficult to reach at this point. However, hypotheses can be pieced together using previous research into similar proteins and mutations, as discussed above. Further research into these mutations would be invaluable to the development and improvement of knowledge surrounding their function and interaction with other cytoskeletal proteins. Although this was out of the scope of this project, the results acquired from these experiments may provide a foundation for future research to expand on.

One limitation of this set of experiments is that they were carried out only in COS-7 cells due to time constraints. To further improve the work completed in this section, repeat transfections are required in other cell lines, such as HaCaTs and C6 cells, with the wild-type and mutated nesprin-3 constructs to establish whether there are any patterns in recruitment ability across a variety of cell lines, including cells in which the mutant constructs show a phenotype.

5. Conclusion

MACF1a3 and nesprin-3 were expressed with varying levels in COS-7, HaCaT, C6 and HDF cells following western blot analysis. Furthermore, they localised differently within COS-7, HaCaT, C6 and HDF cells following immunofluorescence techniques and a uniform pattern of localisation between all the cells for MACF1a3 and nesprin-3 was not found. Although MACF1and nesprin-3 have been shown to interact in co-immunoprecipitation studies, overexpression of nesprin-3 did not achieve MACF1a3 recruitment to the nuclear envelope. Future work may benefit from knockout studies, removing actin and plectin, followed by overexpressing nesprin-3 in different cell lines to assess MACF1a3 recruitment. Lack of MACF1a3 recruitment suggests there may be competition from actin filaments and plectin for binding to nesprin-3.

Plectin binding with nesprin-3 is an association which is specific. Testing wild-type nesprin-3 and two mutant forms of nesprin-3: H222Y and A927E, showed that although a mutation did not result in lack of plectin recruitment, a decreased level of recruitment compared to wild-type nesprin-3. Whilst this study was carried out in COS-7 cells, it would benefit from repeats in different cell lines to assess whether plectin recruitment by the mutant forms of nesprin-3 is affected by other cell types. Finally, investigating MACF1a3 and F-actin association with wild-type nesprin-3 and mutant nesprin-3 constructs in other cell lines would be a useful addition to the development of knowledge in this area.

6. References

Abraham, D. and Burger, A., 2003. *Burger's Medicinal Chemistry Drug Discovery*. London: WileyInterscience.

Adjiri, A., 2016. Identifying and targeting the cause of cancer is needed to cure cancer. *Oncology and Therapy*, 4(1), pp.17-33.

Afghani, N., Mehta, T., Wang, J., Tang, N., Skalli, O. and Quick, Q., 2016. Microtubule actin cross-linking factor 1, a novel target in glioblastoma. *International Journal of Oncology*, 50(1), pp.310-316.

Askeland, D., Fulay, P. and Wright, W., 2011. *The science and engineering of materials*. Stamford, CT: Cengage Learning.

Badano, J., Mitsuma, N., Beales, P. and Katsanis, N., 2006. The ciliopathies: an emerging class of human genetic disorders. *Annual Review of Genomics and Human Genetics*, 7(1), pp.125-148.

Bañuelos, S., Saraste, M. and Carugo, K., 1998. Structural comparisons of calponin homology domains: implications for actin binding. *Structure*, 6(11), pp.1419-1431.

Bernier, G., Mathieu, M., Repentigny, Y., Vidal, S. and Kothary, R., 1996. Cloning and characterization of mouse ACF7, a novel member of the dystonin subfamily of actin binding proteins. *Genomics*, 38(1), pp.19-29.

Bernier, G., Pool, M., Kilcup, M., Alfoldi, J., De Repentigny, Y. and Kothary, R., 2000. Acf7 (MACF) is an actin and microtubule linker protein whose expression predominates in neural, muscle, and lung development. *Developmental Dynamics*, 219(2), pp.216-225.

Bertram, J., 2000. The molecular biology of cancer. *Molecular Aspects of Medicine*, 21(6), pp.167-223.

Bhushan, B., 2010. *Springer Handbook Of Nanotechnology.* Springer. Berlin, p.1174.

Brown, R., Talas, G., Porter, R., McGrouther, D. and Eastwood, M., 1996. Balanced mechanical forces and microtubule contribution to fibroblast contraction. *Journal of Cellular Physiology*, 169(3), pp.439-447.

Burke, B. and Stewart, C., 2012. The nuclear lamins: flexibility in function. *Nature Reviews Molecular Cell Biology*, 14(1), pp.13-24.

Byers, T., Beggs, A., McNally, E. and Kunkel, L., 1995. Novel actin crosslinker superfamily member identified by a two step degenerate PCR procedure. *FEBS Letters*, 368(3), pp.500-504.

Castañón, M., Walko, G., Winter, L. and Wiche, G., 2013. Plectin–intermediate filament partnership in skin, skeletal muscle, and peripheral nerve. *Histochemistry and Cell Biology*, 140(1), pp.33-53.

Chang, L. and Goldman, R., 2004. Intermediate filaments mediate cytoskeletal crosstalk. *Nature Reviews Molecular Cell Biology*, 5(8), pp.601-613.

Chen, H., 2006. The role of microtubule actin cross-linking factor 1 (MACF1) in the Wnt signaling pathway. *Genes & Development*, 20(14), pp.1933-1945.

Crisp, M., Liu, Q., Roux, K., Rattner, J., Shanahan, C., Burke, B., Stahl, P. and Hodzic, D., 2005. Coupling of the nucleus and cytoplasm. *The Journal of Cell Biology*, 172(1), pp.41-53.

Denais, C. and Lammerding, J., 2014. Nuclear mechanics in cancer. *Cancer Biology and the Nuclear Envelope*, pp.435-470.

Denais, C., Gilbert, R., Isermann, P., McGregor, A., te Lindert, M., Weigelin, B., Davidson, P., Friedl, P., Wolf, K. and Lammerding, J., 2016. Nuclear

envelope rupture and repair during cancer cell migration. *Science*, 352(6283), pp.353-358.

Denessiouk, K., Permyakov, S., Denesyuk, A., Permyakov, E. and Johnson, M., 2014. Two structural motifs within canonical EF-Hand calcium-binding domains identify five different classes of calcium buffers and sensors. *PLoS ONE*, 9(10), p.e109287.

Fife, C., McCarroll, J. and Kavallaris, M., 2014. Movers and shakers: cell cytoskeleton in cancer metastasis. *British Journal of Pharmacology*, 171(24), pp.5507-5523.

Fletcher, D. and Mullins, R., 2010. Cell mechanics and the cytoskeleton. *Nature*, 463(7280), pp.485-492.

Fuchs, E. and Karakesisoglou, I., 2001. Bridging cytoskeletal intersections. 15(1), pp.1-14.

Ghasemizadeh, A., Christin, E., Guiraud, A., Couturier, N., Risson, V., Girard, E., Jagla, C., Soler, C., Laddada, L., Sanchez, C., Jaque, F., Garcia, A., Lanfranchi, M., Jacquemond, V., Gondin, J., Courchet, J., Schaeffer, L. and Gache, V., 2019. Skeletal muscle MACF1 maintains myonuclei and mitochondria localization through microtubules to control muscle functionalities. bioRxiv preprint, *Cold Spring Harbor Laboratory doi: https://doi.org/10.1101/636464*

Giakoumettis, D., Kritis, A. and Foroglou, N., 2018. C6 cell line: the gold standard in glioma research. *Hippokratia*, 22(3), pp.105-112.

Gong, T., Besirli, C. and Lomax, M., 2001. MACF1 gene structure: a hybrid of plectin and dystrophin. *Mammalian Genome*, 12(11), pp.852-861.

Gundesli, H., Talim, B., Korkusuz, P., Balci-Hayta, B., Cirak, S., Akarsu, N., Topaloglu, H. and Dincer, P., 2010. Mutation in exon 1f of PLEC, leading to disruption of plectin isoform 1f, causes autosomal-recessive limb-girdle

muscular dystrophy. *The American Journal of Human Genetics*, 87(6), pp.834-841.

Han, E., 1993. A cell cycle and mutational analysis of anchorage-independent growth: cell adhesion and TGF-beta 1 control G1/S transit specifically. *The Journal of Cell Biology*, 122(2), pp.461-471.

Hohmann and Dehghani, 2019. The Cytoskeleton—A Complex Interacting Meshwork. *Cells*, 8(4), p.362.

Hu, L., Su, P., Li, R., Yan, K., Chen, Z., Shang, P. and Qian, A., 2015. Knockdown of microtubule actin crosslinking factor 1 inhibits cell proliferation in MC3T3-E1 osteoblastic cells. *BMB Reports*, 48(10), pp.583-588.

Hu, L., Su, P., Li, R., Yin, C., Zhang, Y., Shang, P., Yang, T. and Qian, A., 2016. Isoforms, structures, and functions of versatile spectraplakin MACF1. *BMB Reports*, 49(1), pp.37-44.

Janin, A., Bauer, D., Ratti, F., Millat, G. and Méjat, A., 2017. Nuclear envelopathies: a complex LINC between nuclear envelope and pathology. *Orphanet Journal of Rare Diseases*, 12(1).

Jefferson, J., Leung, C. and Liem, R., 2004. Plakins: Goliaths that link cell junctions and the cytoskeleton. *Nature Reviews Molecular Cell Biology*, 5(7), pp.542-553.

Jefferson, J., Leung, C. and Liem, R., 2006. Dissecting the sequence specific functions of alternative N-terminal isoforms of mouse bullous pemphigoid antigen 1. *Experimental Cell Research*, 312(15), pp.2712-2725.

Jørgensen, L., Mosbech, M., Færgeman, N., Graakjaer, J., Jacobsen, S. and Schrøder, H., 2014. Duplication in the microtubule-actin cross-linking factor 1 gene causes a novel neuromuscular condition. *Scientific Reports*, 4(1).

Ka, M., Moffat, J. and Kim, W., 2016. MACF1 controls migration and positioning of cortical GABAergic interneurons in mice. *Cerebral Cortex*, 27(12), pp.5525-5538.

Kalluri, R. and Weinberg, R., 2009. The basics of epithelial-mesenchymal transition. *Journal of Clinical Investigation*, 119(6), pp.1420-1428.

Karakesisoglou, I., Yang, Y. and Fuchs, E., 2000. An epidermal plakin that integrates actin and microtubule networks at cellular junctions. *Journal of Cell Biology*, 149(1), pp.195-208.

Katada, K., Tomonaga, T., Satoh, M., Matsushita, K., Tonoike, Y., Kodera, Y., Hanazawa, T., Nomura, F. and Okamoto, Y., 2012. Plectin promotes migration and invasion of cancer cells and is a novel prognostic marker for head and neck squamous cell carcinoma. *Journal of Proteomics*, 75(6), pp.1803-1815.

Ketema, M. and Sonnenberg, A., 2011. Nesprin-3: a versatile connector between the nucleus and the cytoskeleton. *Biochemical Society Transactions*, 39(6), pp.1719-1724.

Ketema, M., Kreft, M., Secades, P., Janssen, H. and Sonnenberg, A., 2013. Nesprin-3 connects plectin and vimentin to the nuclear envelope of Sertoli cells but is not required for Sertoli cell function in spermatogenesis. *Molecular Biology of the Cell*, 24(15), pp.2454-2466.

Ketema, M., Wilhelmsen, K., Kuikman, I., Janssen, H., Hodzic, D. and Sonnenberg, A., 2007. Requirements for the localization of nesprin-3 at the nuclear envelope and its interaction with plectin. *Journal of Cell Science*, 120(19), pp.3384-3394.

Kodama, A., Karakesisoglou, I., Wong, E., Vaezi, A. and Fuchs, E., 2003. ACF7: an essential integrator of microtubule dynamics. *Cell*, 115(3), pp.343-354.

Kodama, A., Karakesisoglou, I., Wong, E., Vaezi, A. and Fuchs, E., 2003. ACF7. *Cell*, 115(3), pp.343-354.

Korenbaum, E., 2002. Calponin homology domains at a glance. *Journal of Cell Science*, 115(18), pp.3543-3545.

Krishnankutty, A., Kimura, T., Saito, T., Aoyagi, K., Asada, A., Takahashi, S., Ando, K., Ohara-Imaizumi, M., Ishiguro, K. and Hisanaga, S., 2017. In vivo regulation of glycogen synthase kinase 3β activity in neurons and brains. *Scientific Reports*, 7(1).

Lee, S. and Dominguez, R., 2010. Regulation of actin cytoskeleton dynamics in cells. *Molecules and Cells*, 29(4), pp.311-325.

Leung, C., Green, K. and Liem, R., 2002. Plakins: a family of versatile cytolinker proteins. *Trends in Cell Biology*, 12(1), pp.37-45.

Leung, C., Sun, D., Zheng, M., Knowles, D. and Liem, R., 1999. Microtubule Actin Cross-Linking Factor (Macf). *The Journal of Cell Biology*, 147(6), pp.1275-1286.

Lin, C., 2005. Microtubule actin crosslinking factor 1b: a novel plakin that localizes to the Golgi complex. *Journal of Cell Science*, 118(16), pp.3727-3738.

Lu, W., Schneider, M., Neumann, S., Jaeger, V., Taranum, S., Munck, M., Cartwright, S., Richardson, C., Carthew, J., Noh, K., Goldberg, M., Noegel, A. and Karakesisoglou, I., 2012. Nesprin interchain associations control nuclear size. *Cellular and Molecular Life Sciences*, 69(20), pp.3493-3509.

Mahanty, S., Dakappa, S., Shariff, R., Patel, S., Swamy, M., Majumdar, A. and Setty, S., 2019. Keratinocyte differentiation promotes ER stress-dependent lysosome biogenesis. *Cell Death & Disease*, 10(4).

May-Simera, H., Gumerson, J., Gao, C., Campos, M., Cologna, S., Beyer, T., Boldt, K., Kaya, K., Patel, N., Kretschmer, F., Kelley, M., Petralia, R., Davey, M. and Li, T., 2016. Loss of MACF1 abolishes ciliogenesis and disrupts apicobasal polarity establishment in the retina. *Cell Reports*, 17(5), pp.1399-1413.

Meinke, P., Nguyen, T. and Wehnert, M., 2011. The LINC complex and human disease. *Biochemical Society Transactions*, 39(6), pp.1693-1697.

Méjat, A., 2010. LINC complexes in health and disease. *Nucleus*, 1(1), pp.40-52.

Miao, Z., Ali, A., Hu, L., Zhao, F., Yin, C., Chen, C., Yang, T. and Qian, A., 2017. Microtubule actin cross-linking factor 1, a novel potential target in cancer. *Cancer Science*, 108(10), pp.1953-1958.

Noreau, A., Bourassa, C., Szuto, A., Levert, A., Dobrzeniecka, S., Gauthier, J., Forlani, S., Durr, A., Anheim, M., Stevanin, G., Brice, A., Bouchard, J., Dion, P., Dupré, N. and Rouleau, G., 2013. SYNE1Mutations in autosomal recessive cerebellar ataxia. *JAMA Neurology*, 70(10) pp. 1296-1300.

Okuda, T., Matsuda, S., Nakatsugawa, S., Ichigotani, Y., Iwahashi, N., Takahashi, M., Ishigaki, T. and Hamaguchi, M., 1999. Molecular cloning of macrophin, a human homologue of drosophila kakapo with a close structural similarity to plectin and dystrophin. *Biochemical and Biophysical Research Communications*, 264(2), pp.568-574.

Ostlund, C., Folker, E., Choi, J., Gomes, E., Gundersen, G. and Worman, H., 2009. Dynamics and molecular interactions of linker of nucleoskeleton and cytoskeleton (LINC) complex proteins. *Journal of Cell Science*, 122(22), pp.4099-4108.

Palmucci, L., Doriguzzi, C., Mongini, T., Restagno, G., Chiado-Piat, L. and Maniscalco, M., 1994. Unusual expression and very mild course of Xp21

muscular dystrophy (Becker type) in a 60-year-old man with 26 percent deletion of the dystrophin gene. *Neurology*, 44(3, Part 1), pp.541-541.

Pegoraro, A., Janmey, P. and Weitz, D., 2017. Mechanical properties of the cytoskeleton and cells. *Cold Spring Harbor Perspectives in Biology*, 9(11), p.a022038.

Pollard, T., 2016. Actin and actin-binding proteins. *Cold Spring Harbor Perspectives in Biology*, 8(8), p.a018226.

Postel, R., Ketema, M., Kuikman, I., de Pereda, J. and Sonnenberg, A., 2011. Nesprin-3 augments peripheral nuclear localization of intermediate filaments in zebrafish. *Journal of Cell Science*, 124(5), pp.755-764.

Quick, Q., 2018. Microtubule-Actin Crosslinking Factor 1 and plakins as therapeutic drug targets. *International Journal of Molecular Sciences*, 19(2), p.368.

Raffaele di Barletta, M., Ricci, E., Galluzzi, G., Tonali, P., Mora, M., Morandi, L., Romorini, A., Voit, T., Orstavik, K., Merlini, L., Trevisan, C., Biancalana, V., Housmanowa-Petrusewicz, I., Bione, S., Ricotti, R., Schwartz, K., Bonne, G. and Toniolo, D., 2000. Different mutations in the LMNA gene cause autosomal dominant and autosomal recessive Emery-Dreifuss muscular dystrophy. *The American Journal of Human Genetics*, 66(4), pp.1407-1412.

Ramaekers, F. and Bosman, F., 2004. The cytoskeleton and disease. *The Journal of Pathology*, 204(4), pp.351-354.

Rezniczek, G., 2003. Plectin 5'-transcript diversity: short alternative sequences determine stability of gene products, initiation of translation and subcellular localization of isoforms. *Human Molecular Genetics*, 12(23), pp.3181-3194.

Sonnenberg, A., Rojas, A. and de Pereda, J., 2007. The structure of a tandem pair of spectrin repeats of plectin reveals a modular organization of the plakin domain. *Journal of Molecular Biology*, 368(5), pp.1379-1391.

Staszewska, I., Fischer, I. and Wiche, G., 2015. Plectin isoform 1-dependent nuclear docking of desmin networks affects myonuclear architecture and expression of mechanotransducers. *Human Molecular Genetics*, 24(25), pp.7373-7389.

Steinböck, F. and Wiche, G., 1999. Plectin: A Cytolinker by Design. *Biological Chemistry*, 380(2), pp.151-158.

Sun, Y., Zhang, J., Kraeft, S., Auclair, D., Chang, M., Liu, Y., Sutherland, R., Salgia, R., Griffin, J., Ferland, L. and Chen, L., 1999. Molecular cloning and characterization of human trabeculin-α, a giant protein defining a new family of actin-binding proteins. *Journal of Biological Chemistry*, 274(47), pp.33522-33530.

Suozzi, K., Wu, X. and Fuchs, E., 2012. Spectraplakins: Master orchestrators of cytoskeletal dynamics. *The Journal of Cell Biology*, 197(4), pp.465-475.

Taranum, S., Sur, I., Müller, R., Lu, W., Rashmi, R., Munck, M., Neumann, S., Karakesisoglou, I. and Noegel, A., 2012. Cytoskeletal interactions at the nuclear envelope mediated by nesprins. *International Journal of Cell Biology*, 2012, pp.1-11.

Valencia, R., Walko, G., Janda, L., Novacek, J., Mihailovska, E., Reipert, S., Andrä-Marobela, K. and Wiche, G., 2013. Intermediate filament-associated cytolinker plectin 1c destabilizes microtubules in keratinocytes. *Molecular Biology of the Cell*, 24(6), pp.768-784.

Wilhelmsen, K., Litjens, S., Kuikman, I., Tshimbalanga, N., Janssen, H., van den Bout, I., Raymond, K. and Sonnenberg, A., 2005. Nesprin-3, a novel outer nuclear membrane protein, associates with the cytoskeletal linker protein plectin. *The Journal of Cell Biology*, 171(5), pp.799-810.

Winter, L., Türk, M., Harter, P., Mittelbronn, M., Kornblum, C., Norwood, F., Jungbluth, H., Thiel, C., Schlötzer-Schrehardt, U. and Schröder, R., 2016. Downstream effects of plectin mutations in epidermolysis bullosa simplex with muscular dystrophy. *Acta Neuropathologica Communications*, 4(1).

Yang, J. and Weinberg, R., 2008. Epithelial-Mesenchymal Transition: At the crossroads of development and tumor metastasis. *Developmental Cell*, 14(6), pp.818-829.

Yucel, G. and Oro, A., 2011. Cell Migration: GSK3β steers the cytoskeleton's tip. *Cell*, 144(3), pp.319-321.

Zaoui, K., Benseddik, K., Daou, P., Salaun, D. and Badache, A., 2010. ErbB2 receptor controls microtubule capture by recruiting ACF7 to the plasma membrane of migrating cells. *Proceedings of the National Academy of Sciences*, 107(43), pp.18517-18522.